
The Mixtures and the Neural Critics: On the Pointwise Mutual Information Profiles of Fine Distributions

Paweł Czyż^{*1,2}Frederic Grabowski^{*3}Julia E. Vogt^{4,5}Niko Beerenwinkel^{†1,5}Alexander Marx^{†2,4}¹Department of Biosystems Science and Engineering, ETH Zurich ²ETH AI Center, ETH Zurich³Institute of Fundamental Technological Research, Polish Academy of Sciences⁴Department of Computer Science, ETH Zurich ⁵SIB Swiss Institute of Bioinformatics

Abstract

Mutual information quantifies the dependence between two random variables and remains invariant under diffeomorphisms. In this paper, we explore the pointwise mutual information profile, an extension of mutual information that maintains this invariance. We analytically describe the profiles of multivariate normal distributions and introduce the family of *fine distributions*, for which the profile can be accurately approximated using Monte Carlo methods. We then show how fine distributions can be used to study the limitations of existing mutual information estimators, investigate the behavior of neural critics used in variational estimators, and understand the effect of experimental outliers on mutual information estimation. Finally, we show how fine distributions can be used to obtain model-based Bayesian estimates of mutual information, suitable for problems with available domain expertise in which uncertainty quantification is necessary.

1 INTRODUCTION

Mutual information (MI) is a non-parametric statistical measure used to determine the dependency between two random variables (r.v.) and numerous approaches have been proposed to estimate it (Kay, 1992; Kraskov et al., 2004; Cellucci et al., 2005; Belghazi

et al., 2018). In recent work, Czyż et al. (2023) proposed a family of distributions for which ground-truth MI is analytically tractable to evaluate the performance of selected estimators on different distributions. They concluded that there is no universally acclaimed state-of-the-art estimator, with different methods performing best under different assumptions on the data-generating process, which had been often implicitly assumed. In parametric statistics, generative models are used to explicitly state the assumptions about the data-generating process. Although such model-based estimators have been used in settings with discrete r.v. (Hutter, 2001; Brillinger, 2004), the only model-based MI estimator for continuous r.v. is canonical correlation analysis (CCA), proposed by Kay (1992) and Brillinger (2004). As CCA assumes that the joint distribution is multivariate normal, we consider the development of more advanced model-based MI estimators to be an important open problem.

A second and related problem is the construction of new distributions with known ground-truth MI, which can be used to assess the performance of different estimators under varying distributional assumptions. Czyż et al. (2023) used multivariate normal and Student distributions (and their transformations) with analytically tractable MI to model the sparsity of interactions and effects of long tails. However, these distributions are far from universal: they are not suitable to model communication channels in which experimental failures result in measurement outliers or distributions used in biology (Grabowski et al., 2019) and physics (Carrara & Ernst, 2023), which involve both continuous and discrete r.v. Moreover, reparametrizations with diffeomorphisms do not change the pointwise mutual information profile (the distribution of pointwise mutual information), limiting the expressivity of constructed distributions.

^{*}Joint first author [†]Joint supervision

In this work, we address both problems: we propose a family of *fine distributions* for which the ground-truth MI can be reliably estimated using Monte Carlo methods with arbitrarily high accuracy. The proposed distributions include normalizing flows (Kobyzev et al., 2021; Papamakarios et al., 2021) and their finite mixtures, allow for discrete and continuous random variables, and can be used to investigate the phenomena involving outliers resulting from failed experimental measurements. Moreover, we show how they can be used to create expressive generative models which provide model-based mutual information estimates, beyond the linear case of CCA.

Contributions We introduce a novel family of fine distributions, for which mutual information and the pointwise mutual information profile can be accurately determined using Monte Carlo methods (Sec. 2). In Sec. 3 we demonstrate three different applications of fine distributions: first, we show how to construct low-dimensional distributions posing significant challenges to existing mutual information estimators (Sec. 3.1). Second, we use the introduced family of fine distributions to study the robustness of mutual information estimators to inliers and outliers (Sec. 3.2). Third, we show how to apply fine distributions to understand the biases and sample efficiency of variational estimator employing neural critics (Sec. 3.3). Finally, we demonstrate how the introduced family of fine distributions can be used to provide model-based mutual information estimates (Sec. 4), allowing for Bayesian inference of mutual information.

2 THEORETICAL FRAMEWORK

In this paper, we consider random variables valued in smooth manifolds without boundary (Lee, 2012, Ch. 1) equipped with given reference measures. In particular, our results apply to both categorical and continuous random variables, as the considered manifolds include open subsets of the Euclidean space \mathbb{R}^n (equipped with the Lebesgue measure) as well as zero-dimensional discrete spaces $\{1, \dots, m\}$ (equipped with the counting measure). For a given pair of smooth manifolds \mathcal{X} and \mathcal{Y} , we equip their product $\mathcal{X} \times \mathcal{Y}$ with the product measure and define the set $\mathcal{P}(\mathcal{X}, \mathcal{Y})$ to consist of all probability measures P_{XY} on $\mathcal{X} \times \mathcal{Y}$ such that the measures P_{XY} , $P_X(A) = P_{XY}(A \times \mathcal{Y})$ and $P_Y(B) = P_{XY}(\mathcal{X} \times B)$ have smooth and positive PDFs (or PMFs) p_{XY} , p_X and p_Y with respect to the reference measures on $\mathcal{X} \times \mathcal{Y}$, \mathcal{X} and \mathcal{Y} , respectively. The primary reason for studying $\mathcal{P}(\mathcal{X}, \mathcal{Y})$ is a convenient formula for pointwise mutual information (Pinsker & Feinstein, 1964, Ch. 2):

Definition 1 (Pointwise Mutual Information). *Let X*

and Y be random variables valued in \mathcal{X} and \mathcal{Y} , respectively, such that $P_{XY} \in \mathcal{P}(\mathcal{X}, \mathcal{Y})$. The pointwise mutual information (PMI) is defined¹ as

$$\text{PMI}_{XY}(x, y) = \log \frac{p_{XY}(x, y)}{p_X(x)p_Y(y)}.$$

Note that from smoothness and positivity of all the densities it follows that PMI is a smooth, hence measurable, function, s.t. the following distribution exists:

Definition 2 (PMI profile). *The pointwise mutual information profile² Prof_{XY} is defined as the distribution of the random variable $T = \text{PMI}_{XY}(X, Y)$.*

The mutual information is the first moment of the profile, $\mathbf{I}(X; Y) = \mathbb{E}_{T \sim \text{Prof}_{XY}}[T]$, and is known to be invariant under diffeomorphisms (Kraskov et al., 2004, Appendix). More generally, in Appendix A.1 we show that the whole profile is invariant (see Fig. 1):

Theorem 3. *Let $P_{XY} \in \mathcal{P}(\mathcal{X}, \mathcal{Y})$ and $f: \mathcal{X} \rightarrow \mathcal{X}$ and $g: \mathcal{Y} \rightarrow \mathcal{Y}$ be diffeomorphisms. Then for $X' = f(X)$ and $Y' = g(Y)$ it holds that $P_{X'Y'} \in \mathcal{P}(\mathcal{X}, \mathcal{Y})$ and $\text{Prof}_{XY} = \text{Prof}_{X'Y'}$.*

In Appendix A.2 we prove the following three results, characterizing the profiles of simple distributions:

Proposition 4. *Let X and Y be r.v. with joint distribution $P_{XY} \in \mathcal{P}(\mathcal{X}, \mathcal{Y})$. Then, $\mathbf{I}(X; Y) = 0$ if and only if $\text{Prof}_{XY} = \delta_0$ is the Dirac measure with a single atom at 0.*

Proposition 5. *If X and Y are discrete r.v. with $P_{XY} \in \mathcal{P}(\mathcal{X}, \mathcal{Y})$, then the PMI profile is discrete:*

$$\text{Prof}_{XY} = \sum_{x \in \mathcal{X}} \sum_{y \in \mathcal{Y}} p_{XY}(x, y) \delta_{\text{PMI}_{XY}(x, y)}.$$

Theorem 6. *Let X and Y be r.v. such that the joint distribution $P_{XY} \in \mathcal{P}(\mathbb{R}^m, \mathbb{R}^n)$ is multivariate normal. If $k = \min(m, n)$ and $\rho_1, \rho_2, \dots, \rho_k$ are canonical correlations (Jendoubi & Strimmer, 2019) between X and Y , then the profile Prof_{XY} is a generalized χ^2 distribution, namely the distribution of the variable*

$$T = \mathbf{I}(X; Y) + \sum_{i=1}^k \frac{\rho_i}{2} (Q_i - Q'_i),$$

where Q_i and Q'_i are i.i.d. variables sampled according to the χ_1^2 distribution. In particular, Prof_{XY} is symmetric around its median, which coincides with

¹We use the natural logarithm, meaning that all quantities are measured in nats.

²Although we are not aware of a prior formal definition and studies of the PMI profile, histograms of approximate PMI between words have been studied before in the computational linguistics community (Allen & Hospedales, 2019).

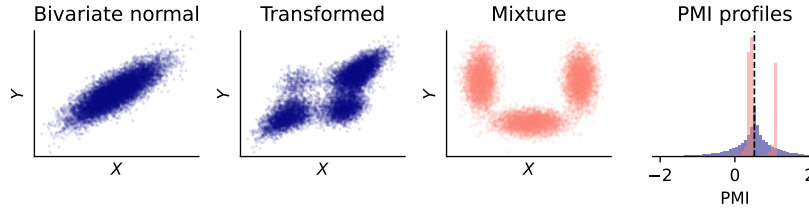


Figure 1: First two panels: samples from a bivariate normal distribution and a transformed distribution. Both distributions have the same PMI profile (blue histogram in the fourth panel). Third panel: mixture distribution with distinct PMI profile, which cannot be obtained as a transformation of multivariate normal distribution due to a different PMI profile (pink histogram in the fourth panel). All three distributions have the same mutual information, marked with the black line in the fourth panel.

the mean $\mathbf{I}(X;Y) = -\frac{1}{2} \sum_{i=1}^k \log(1 - \rho_i^2)$, and all the moments of this distribution exist; its variance is equal to $\rho_1^2 + \dots + \rho_k^2$.

However, analytic formulae governing PMI profiles are not known except for the simplest cases above and their reparametrizations by diffeomorphisms due to Theorem 3. Below we show how to construct a family of distributions with diverse PMI profiles, for which the PMI profile can be approximated numerically.

Definition 7. We call a distribution $P_{XY} \in \mathcal{P}(\mathcal{X}, \mathcal{Y})$ fine if it is possible to sample $(X, Y) \sim P_{XY}$ and for every point $(x, y) \in \mathcal{X} \times \mathcal{Y}$ we can analytically evaluate the densities $p_{XY}(x, y)$, $p_X(x)$ and $p_Y(y)$.

For example, discrete distribution as well as multivariate normal and Student distributions are fine. With the advancements in probabilistic computation, we can expect that the list of known fine distributions will grow over time.

The properties are chosen so that we can estimate the PMI profile and mutual information with Monte Carlo approaches. Namely, observe that it is easy to sample $T \sim \text{Prof}_{XY}$ by sampling a data point (x, y) and evaluating $t = \text{PMI}_{XY}(x, y)$. Then, MI can be approximated with a Monte Carlo estimate of the integral $\mathbf{I}(X;Y) = \mathbb{E}[T]$. Assuming $\mathbf{I}(X;Y) < \infty$, the Monte Carlo estimator of the mutual information is guaranteed to be unbiased. For a detailed discussion of Monte Carlo standard error (MCSE) under different regularity conditions see Flegal et al. (2008).

Analogously, to estimate the PMI profile, we can approximate it with a histogram: for bin $B \subset \mathbb{R}$ one can introduce its indicator function $\mathbf{1}_B$ and integrate $\mathbb{E}[\mathbf{1}_B(T)]$. Its cumulative density function can be approximated with an empirical sample using the expectations $\mathbb{E}[\mathbf{1}_{(-\infty, a_n]}(T)]$ for a given sequence (a_n) . As the characteristic functions are bounded between 0 and 1, the Monte Carlo estimator of both quantities is unbiased and has standard error bounded from above by $1/\sqrt{4n}$ due to the inequality of Popoviciu (1935).

We can enlarge the family of known fine distributions with two constructions, with proofs given in Appendix A.4. First, we can transform known fine distributions with diffeomorphisms with tractable Jacobians, such as normalizing flows (Papamakarios et al., 2021; Kobyzev et al., 2021):

Proposition 8. If P_{XY} is fine and f and g are diffeomorphisms with tractable Jacobians, then $P_{f(X)g(Y)}$ is fine.

As noted in Theorem 3, the above construction does not change the PMI profile. However, it is possible to obtain more expressive profiles by using finite mixtures of fine distributions (see Fig. 1):

Proposition 9. Consider a mixture distribution $P_{X'Y'}$ with weights w_1, \dots, w_K and component distributions $P_{X_1Y_1}, \dots, P_{X_KY_K}$. If all component distributions are fine, then also the mixture distribution is fine.

Since Gaussian mixture models are universal approximators of smooth densities, and they belong to the fine distribution family, in principle one could use these constructions to approximate any distribution. In practice, the evaluation time of PMI grows linearly with the number of components and can become costly for a high number of components (or when large normalizing flow architectures are used). We consider estimating mutual information of mixture distributions an important problem due to their counterintuitive ability to create and destroy information (Haussler & Opper, 1997; Kolchinsky & Tracey, 2017):

Proposition 10. Consider r.v. (X_k, Y_k) such that $\mathbf{I}(X_k; Y_k) < \infty$ for $k = 1, \dots, K$ and their mixture (X', Y') with weights w_1, \dots, w_K . The following inequalities apply:

$$0 \leq \mathbf{I}(X'; Y') \leq \log K + \sum_{k=1}^K w_k \mathbf{I}(X_k; Y_k).$$

Moreover, these inequalities are tight:

1. There exists a mixture such that $\mathbf{I}(X'; Y') = \log K$ even though $\mathbf{I}(X_k; Y_k) = 0$ for all k .

-
2. *There exists a mixture such that $\mathbf{I}(X'; Y') = 0$ even though $\mathbf{I}(X_k; Y_k) > 0$ for all k .*

For completeness, we include a proof in Appendix A.6.

3 CASE STUDIES

In this section, we apply fine distributions to three distinct problems. In Sec. 3.1 we demonstrate how they can be used to extend existing benchmarks of mutual information estimators. In Sec. 3.2 we show how fine can be used in experimental sciences to investigate the robustness of mutual information to outliers and inliers. In Sec. 3.3 we apply fine to investigate the biases and sample efficiency of variational estimators employing neural critics.

3.1 Extending the Benchmarks

In this section, we show how expressive the fine distributions are by visualizing them and demonstrate how they can be applied to investigate the limits of the applicability of mutual information estimators. Czyż et al. (2023) benchmarked mutual information estimators using r.v. (X, Y) distributed according to multivariate normal and Student distributions (for which mutual information is analytically tractable Arellano-Valle et al. (2013)) and their transformations $(f(X), g(Y))$, where f and g are continuous injective functions (which ensures that $\mathbf{I}(f(X); g(Y)) = \mathbf{I}(X; Y)$).

However, transforming only multivariate normal and Student distributions does not ensure that the family of distributions is diverse enough. In particular, if f and g were diffeomorphisms, the diversity of the PMI profiles would be very limited due to Theorem 3. The proposed family of fine distributions can be used as a more expressive alternative to the multivariate normal and Student distributions. Although the analytical formula for ground-truth mutual information of fine distributions is not available, it can be reliably estimated with a Monte Carlo estimator.

To illustrate this application, we implemented four low-dimensional distributions in TensorFlow Probability on JAX (Dillon et al., 2017; Bradbury et al., 2018) assuming that X and Y are valued in Euclidean spaces. Additionally, in Appendix B, we consider cases involving discrete variables. We visualise samples from the distributions considered in Fig. 2 and defer the detailed description to Appendix C.1; the X distribution is a mixture of two bivariate normal distributions. The marginal distributions P_X and P_Y are normal, although the joint distribution P_{XY} is not. The AI distribution is a mixture of six bivariate normal

distributions, illustrating how expressive fine distributions can be. To illustrate that fine distributions are more expressive than mixtures of normal distributions, we consider a two-dimensional X variable and a one-dimensional Y variable. The Waves distribution was created using twelve multivariate normal distributions in which the X variable has been transformed by a diffeomorphism. The Galaxy distribution was created using two multivariate normal distributions in which the X variable was transformed with the spiral diffeomorphism (Czyż et al., 2023).

Analogous distributions could be also defined in higher dimensions or transformed via continuous injections, which preserve mutual information. We do not aim to create a rigorous benchmark in this work, so we restricted our attention only to these four distributions, and for each of them we sampled ten data sets with $N = 5000$ points and applied five estimators: the histogram-based estimator (Cellucci et al., 2005; Darbellay & Vajda, 1999), the popular KSG estimator (Kraskov et al., 2004), canonical correlation analysis (Kay, 1992; Brillinger, 2004) and two neural estimators: InfoNCE (Oord et al., 2018) and MINE (Belghazi et al., 2018) (see Appendix C.2 for hyperparameters used). The estimates are shown in Fig. 2.

Even though the considered problems are low-dimensional and do not encode more information than 1.5 nats, they pose a considerable challenge for the estimators. The performance of the KSG estimator is consistently the best one, with the Waves task not solved by any estimator. The CCA estimator, excelling at distributions that are close to multivariate normal (Czyż et al., 2023), is not able to capture any information at all. This suggests that fine distributions can provide a rich set of distributions that can be used to test mutual information estimators.

3.2 Modeling Outliers

In this section, we use fine distributions to study the effect of inliers and outliers on mutual information estimation. Consider an electric circuit or a biological system modeled as a communication channel $p_{Y|X}(y | x)$. The researcher controls the input variable X , which results in a distribution P_X , and subsequently measures the outcome variable Y . The mutual information $\mathbf{I}(X; Y)$ is then estimated based on the collected experimental samples (Nałęcz-Jawecki et al., 2023).

However, every experimental system can suffer from occasional failures. We model the output of a failing system with a noise distribution with a PDF $n(y)$. If the probability of system failure does not depend on input value x , the communication channel becomes a

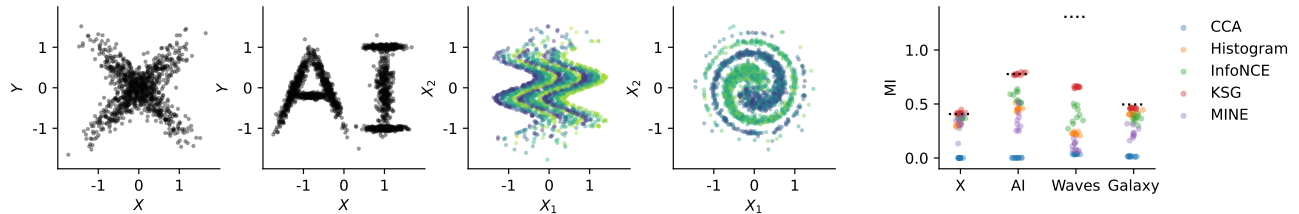


Figure 2: Samples from the proposed distributions. Distributions X and AI represent one-dimensional variables X and Y . Distributions Waves and Galaxy plot two-dimensional X variable using spatial coordinates, while one-dimensional Y variable is represented by color. The rightmost plot presents estimates according to different mutual information algorithms using independently generated data sets with $N = 5000$ points each, compared to the ground-truth mutual information of the distribution (dotted line).

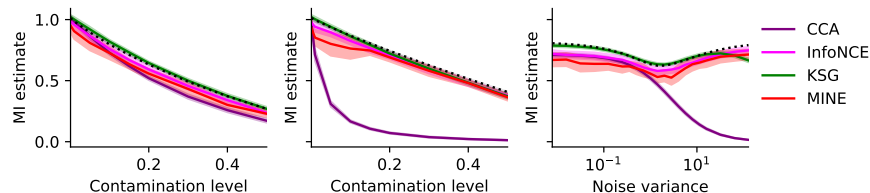


Figure 3: Left: increasing the contamination level α with inlier noise distribution (covariance of $N_{\tilde{Y}}$ is of similar scale as the signal distribution P_{XY}). Middle: increasing the contamination level α with outlier noise distribution (noise covariance $N_{\tilde{Y}}$ has 5^2 larger scale than the signal distribution P_{XY}). Right: increasing the variance of the noisy normal distribution for constant contamination of 20%. Note that outliers (corresponding to very small or large covariance of $n(y)$) have less impact than inliers (corresponding to covariance of $n(y)$ similar to the covariance of the signal distribution P_{XY}).

mixture:

$$p_{Y'|X}(y | x) = (1 - \alpha)p_{Y|X}(y | x) + \alpha n(y).$$

By multiplying both sides by the density $p_X(x)$, the distribution of the channel inputs provided by the scientist, we arrive at the mixture distribution $P_{XY'}$ with PDF

$$p_{XY'}(x, y) = (1 - \alpha)p_{XY}(x, y) + \alpha n(y)p_X(x).$$

If the system failure is unnoticed, one can only measure the r.v. Y' , rather than Y . It is therefore of interest to understand how much $\mathbf{I}(X; Y)$ and $\mathbf{I}(X; Y')$ can differ under realistic assumptions on the noise $n(y)$ and whether the standard mutual information estimation techniques are robust to it. In Appendix A.3 we prove the following upper bound:

Proposition 11. Consider variables X , Y and Y' , such that

$$p_{XY'}(x, y) = (1 - \alpha)p_{XY}(x, y) + \alpha n(y)p_X(x)$$

with contamination level $\alpha \in [0, 1]$. Then,

$$\mathbf{I}(X; Y') \leq (1 - \alpha)\mathbf{I}(X; Y).$$

However, we can use fine distributions to evaluate this quantity exactly. We consider a setting with a two-dimensional input variable X and two-dimensional output variables Y (perfect output) and Y' (contaminated output). As the joint density p_{XY} we used a multivariate normal with unit scale and correlations $\text{corr}(X_1, Y_1) = \text{corr}(X_2, Y_2) = 0.8$ and for the noise $n(y)$ we used a multivariate normal distribution with covariance $\sigma^2 I_2$. If $\sigma^2 \approx 1$ this results in inliers, where the noise distribution is hard to distinguish from the signal. For $\sigma^2 \ll 1$ the system failures are all close to 0, while outliers are present for $\sigma^2 \gg 1$.

In Fig. 3 we present the results of three experiments: in the first two, we changed the contamination level $\alpha \in [0, 0.5]$ for $\sigma^2 = 1$ (inlier noise) and $\sigma^2 = 5^2$ (outlier noise) respectively. In the third experiment, we fixed $\alpha = 0.2$ and varied $\sigma^2 \in [2^{-7}, 2^8]$. We see that the inlier noise results in a slightly faster decrease of mutual information, while the outlier noise decreases almost linearly following the upper bound $(1 - \alpha)\mathbf{I}(X; Y)$. Interestingly, in this low-dimensional setting, the KSG, MINE, and InfoNCE estimators reliably estimate the mutual information $\mathbf{I}(X; Y')$, which can significantly differ from $\mathbf{I}(X; Y)$. Although CCA would be the preferred method to estimate $\mathbf{I}(X; Y)$

without any noise (Czyż et al., 2023), even a small number of outliers ($\alpha = 5\%$) can result in unreliable estimates.

3.3 Understanding Neural Critics

Variational estimators of mutual information optimize a critic $f: \mathcal{X} \times \mathcal{Y} \rightarrow \mathbb{R}$ to obtain an approximate lower bound on mutual information. For example, the Donsker–Varadhan variational approximation (Belhazi et al., 2018)

$$I_{\text{DV}} = \sup_f (\mathbb{E}_{P_{XY}}[f] - \log \mathbb{E}_{P_X \otimes P_Y}[\exp f])$$

is a lower bound and $I_{\text{DV}} = \mathbf{I}(X; Y)$ whenever $f = \text{PMI}_{XY} + c$ for any real number c . Analogously, the lower bound of Nguyen et al. (2007),

$$I_{\text{NWJ}} = \sup_f (\mathbb{E}_{P_{XY}}[f] - \mathbb{E}_{P_X \otimes P_Y}[\exp(f - 1)]),$$

becomes tight for $f = \text{PMI}_{XY} + 1$. Oord et al. (2018) propose a variational approximation loss which uses a batch of $(x_i, y_i)_{i=1, \dots, n}$ samples from P_{XY} to estimate

$$I_{\text{NCE}}(f) = \mathbb{E} \left[\frac{1}{n} \sum_{i=1}^n \log \frac{\exp f(x_i, y_i)}{\frac{1}{n} \sum_{j=1}^n \exp f(x_i, y_j)} \right]$$

Here, if $f(x, y) = \text{PMI}_{XY}(x, y) + c(x)$, where c is any function, then $I_{\text{NCE}}(f) \rightarrow \mathbf{I}(X; Y)$ as $n \rightarrow \infty$.

In practice, only a finite sample is available, so expectation values are only approximate (and any particular finite-sample estimate does not need to be a lower bound on mutual information) and critic f is modeled via some parametric family, for example, a neural network, which has to be learned from the data available. It is therefore of interest to understand the finite-sample behavior of neural critics and variational approximations.

Do learned critics capture PMI well? We simulated $N = 5000$ data points from a mixture of four bivariate normal distributions (Fig. 4) with $\mathbf{I}(X; Y) = 0.36$ and fitted the neural critic (see Appendix C) to half of the data retaining the latter half as the test data set, on which the final loss value was evaluated, yielding $I_{\text{NWJ}} = 0.33$, $I_{\text{DV}} = 0.32$, $I_{\text{NCE}} = 0.35$, which have about 10% error compared to the ground-truth. This difference can be attributed to the critic being misspecified or the estimation error due to evaluation on a finite batch. In Fig. 4 we plot the critic and the PMI. As the Donsker–Varadhan estimator estimates PMI only up to an additive constant, we normalized the critic and the PMI plots to have zero mean. Analogously, we removed the functional degree of freedom $c(x)$ from the InfoNCE estimator by removing the mean calculated along the y dimension. Overall we saw a mismatch, suggesting that neural critics do not capture

the PMI function of the distribution well. However, we can compare the PMI profile with the histogram of the values predicted by the critic in Fig. 4 (shifting the PMI profile and the histogram to have mean 0 for the Donsker–Varadhan estimator). For InfoNCE it is not possible to compare the PMI profile with the critic values due to the functional degree of freedom $c(x)$. Generally, we see little discrepancy between the (shifted) PMI profile and learned values. This suggests that although the neural critics may not learn the PMI function properly in regions with low density, the PMI profile can be still approximated well.

How robust are the estimators to a misspecified critic? In the next experiment (Fig. 5), we evaluated I_{DV} , I_{NWJ} , I_{InfoNCE} , and the simple Monte Carlo estimator (MC) for increasing sample sizes where we provided them with an oracle critic f . Using a perfect critic, $f = \text{PMI}_{XY}$, we saw that all estimators had similar performance on this problem. When a constant bias was added, $f = \text{PMI}_{XY} + c$, the Monte Carlo and NWJ estimators became biased. Finally, InfoNCE was the only unbiased estimator when a functional degree of freedom was added, $f(x, y) = \text{PMI}_{XY}(x, y) + \sin(x^2)$.

In low dimensions, variational approximations do not provide worse mutual information values than the Monte Carlo estimator, when the correct critic function is used, and are more robust to misspecification due to additional degrees of freedom. However, this additional robustness results in a bias in higher dimensions. We simulated a data set using a multivariate normal distribution with 25 strongly interacting components, $\text{corr}(X_i, Y_i) = 0.8$, which results in $\mathbf{I}(X; Y) \approx 12.8$. Although the Monte Carlo estimator and NWJ estimator (which are not robust to additional degrees of freedom) provided estimates close to the ground-truth (with Monte Carlo slightly outperforming NWJ in both bias and variance), Donsker–Varadhan estimator resulted in a strong positive bias for small batch sizes and InfoNCE had a negative bias with very low variance.

4 MODEL-BASED ESTIMATION

As the final application of fine distributions, we consider the problem of model-based estimation of mutual information. Consider a parametric statistical model $\{P_\theta \mid \theta \in \Theta\}$ for (X, Y) such that for every value of the parameter vector θ the mutual information contained in P_θ is known. That is, we define $\mathbf{I}(P_\theta) := \mathbf{I}(X; Y)$, where $(X, Y) \sim P_\theta$.

If the data are modeled as i.i.d. r.v. $(X_i, Y_i) \sim P_\theta$, one can estimate θ and use $\mathbf{I}(P_\theta)$ as an estimate of the mutual information. For example, Brillinger (2004) inter-

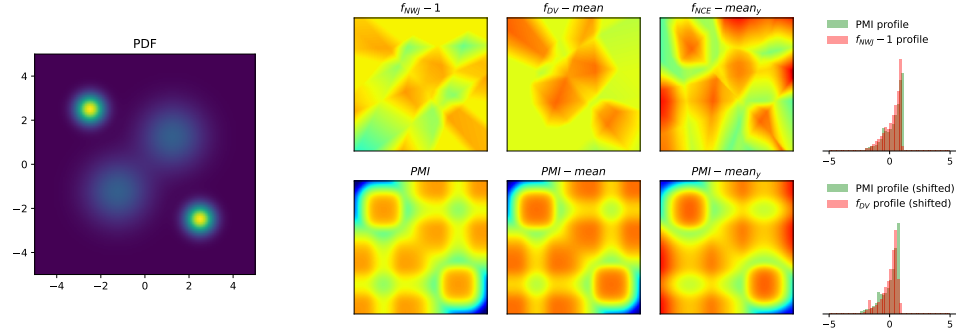


Figure 4: Left: PDF of the considered distribution. Middle: neural critic and PMI values. Right: normalized neural critic and PMI profiles.

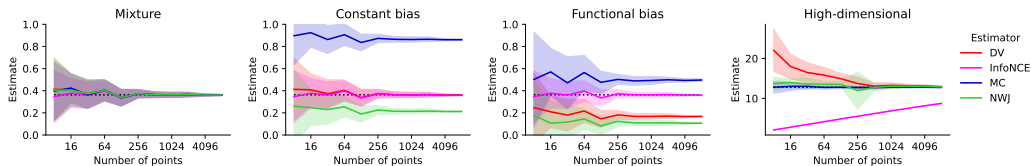


Figure 5: Estimation of mutual information using a function approximating PMI as a function of sample size for Monte Carlo (MC), InfoNCE, Donsker-Varadhan and NWJ losses. From left to right: true PMI function is used, a constant bias is added, a functional bias is added. The rightmost plot: true PMI function is used in a high-dimensional problem.

pretends the CCA estimator (Kay, 1992) as the estimate $\mathbf{I}(P_{\hat{\theta}})$, where $\hat{\theta}$ is the maximum likelihood estimate in the model in which P_{θ} is a multivariate normal distribution. Analogously, if X_i and Y_i are discrete r.v., one can model θ as a probability matrix and assume P_{θ} to be the multinomial distribution. Brillinger (2004) proposes to use the maximum likelihood estimate $\hat{\theta}$ also in this case to provide the estimate $\mathbf{I}(P_{\hat{\theta}})$.

More generally, Hutter (2001) observes that if the Dirichlet prior is used for θ , the Bayesian posterior $P(\theta | X_1, Y_1, \dots, X_N, Y_N)$ will also be a Dirichlet distribution and provides an approximation via moments to the posterior distribution of mutual information.

We note that one can construct a Bayesian alternative for the CCA estimator by using a prior on the covariance matrix (Lewandowski et al., 2009; Legramanti et al., 2020) and Markov chain Monte Carlo (Gelman et al., 2013, Ch. 11) to provide samples $\theta_1, \dots, \theta_M$ from the posterior $P(\theta | X_1, Y_1, \dots, X_N, Y_N)$ and construct a sample-based approximation to the posterior on mutual information, $\mathbf{I}(P_{\theta_1}), \dots, \mathbf{I}(P_{\theta_M})$.

More generally, consider a statistical model $\{P_{\theta} | \theta \in \Theta\}$ such that all P_{θ} are fine distributions. One can again find maximum likelihood $\hat{\theta}$ or, if prior $P(\theta)$ is used, apply Bayesian inference algorithms to construct a sample $\theta_1, \dots, \theta_M$ from the posterior. Although the exact values for $\mathbf{I}(P_{\hat{\theta}})$ and $\mathbf{I}(P_{\theta_1}), \dots, \mathbf{I}(P_{\theta_M})$ are not available, they can be approximated as in Sec. 2. Since

fine distributions include mixture models and normalizing flows, this approach can be used as a general technique for building model-based mutual information estimators, where the generative model can be constructed using domain knowledge. Moreover, this is the first Bayesian estimator of the PMI profile: as all distributions P_{θ_m} are fine, one can construct M histograms (or CDFs) approximating the profile.

To illustrate this approach we implemented a sparse Gaussian mixture model (see Appendix D) in NumPyro (Phan et al., 2019) and used the NUTS sampler (Hoffman & Gelman, 2014) to obtain a Bayesian posterior conditioned on 500 data points from the AI distribution (see Fig. 6). We see that the posterior is concentrated around the ground-truth mutual information value and the ground-truth PMI profile is well-approximated by the posterior samples.

However, this method relies on a model of the true data-generating distribution. As observed in Sec. 3.1, the CCA estimator can yield unreliable estimates when the model is misspecified, that is, the true data-generating process P_{XY} does not belong to the assumed multivariate normal family P_{θ} (Watson & Holmes, 2016). To illustrate the risks of using misspecified models, we applied the same Gaussian mixture model to 500 points from the Galaxy distribution (Fig. 6). We see that a data sample simulated from the model looks substantially different from the

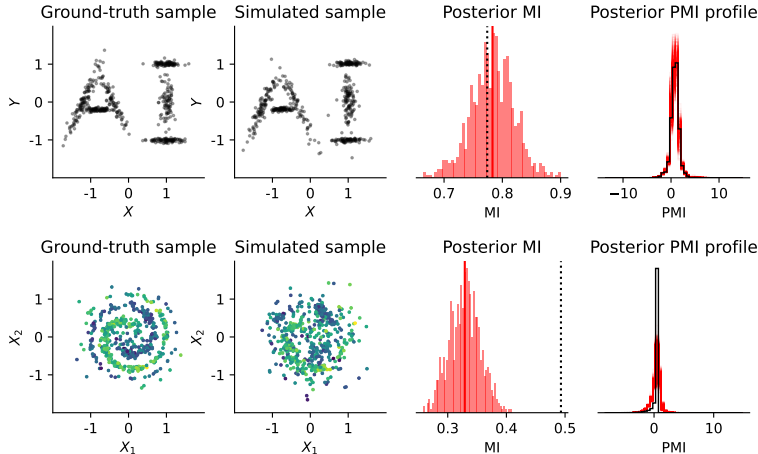


Figure 6: From left to right: sample from the true data distribution, data distribution sampled using a single MCMC sample, posterior distribution of the mutual information (black line denotes ground-truth value), and posterior distribution of the PMI profiles (black curve denotes the ground-truth value). Top row: well-specified model for the AI distribution. Bottom row: misspecified model for the Galaxy distribution results in biased inferences with miscalibrated posterior. Posterior predictive checking can be used to diagnose unreliable estimates.

observed data, meaning that the model did not capture the distribution well. In particular, most of the probability mass of the Bayesian posterior is far from the ground-truth mutual information. Similarly, the posterior on the PMI profile is biased. We therefore recommend using model-checking techniques such as posterior predictive checks (Gelman et al., 2013, Ch. 6) and discriminator-based validation (Sankaran & Holmes, 2023, Sec. 4) to understand the deficiencies of the model. To mitigate the risk of overfitting, which can bias the model (see Appendix D), we recommend cross-validation (Piironen & Vehtari, 2017).

5 CONCLUSION

In this article, we have studied pointwise mutual information profiles, determining them analytically for multivariate normal distributions (Theorem 6), and proposed the family of fine distributions, which include multivariate normal and Student distributions, mixture models and normalizing flows, for which the profile can be approximated using Monte Carlo methods. We showed how fine distributions can be used to provide novel benchmark tasks to test mutual information estimators and calculate mutual information transmitted through a communication channel in the presence of inliers and outliers (which can be used in the experimental design in electrical and biological sciences). Fine distributions allowed us to study how well neural critics approximate pointwise mutual information and we conclude that the error in low-dimensional settings can originate from neural critic misspecification, rather than the formula used to provide a variational

approximation. Finally, we showed how Bayesian estimates of mutual information between continuous r.v. can be performed using fine distributions. Additionally, the proposed method provides estimates of the pointwise mutual information profiles, which can be more accurate than the ones obtained using neural critics and variational lower bounds. Although this approach is not universal, we find it suitable for problems with precise domain knowledge available (which can be used to construct the generative distribution P_θ and provide the prior $P(\theta)$) and in which uncertainty quantification is desired.

Limitations and Further Research In Sec. 3.2, we study a channel in which the probability of failure α is constant and independent of the input variable X . However, in both biological and electric systems this assumption may be broken: for large values of x the system may result in an outlier more easily. However, if α depends on x , it is not straightforward to use fine distributions to model these situations. Although we propose fine distributions as a basis for model-based Bayesian inference of mutual information, model misspecification (Watson & Holmes, 2016) as well as underfitting and overfitting can bias inference (Piironen & Vehtari, 2017). We therefore recommend following Gelman et al. (2020) to carefully validate the model. Overfitting and model misspecification may be more difficult to detect especially in high-dimensional situations or when more expressive models are constructed, for example using normalizing flows, as Bayesian inference for models involving neural networks is known to be challenging (Izmailov et al., 2021). Finally, fine

distributions could be used to study sample size requirements and optimality of different estimation techniques under different distributional assumptions similarly as in Czyż et al. (2023). However, in this work we do not construct a formal benchmark (cf. Sec. 3.1), leaving it for future work. In particular, fine distributions provide a general framework for problems involving both continuous and discrete r.v. and it would be interesting to consider computational examples using other manifolds, for example by using computational geometry frameworks such as `geomstats` (Milane et al., 2020).

Acknowledgments

FG was supported by the Norwegian Financial Mechanism GRIEG-1 grant operated by Narodowe Centrum Nauki (National Science Centre, Poland) 2019/34/H/NZ6/00699. PC and AM were supported by a fellowship from the ETH AI Center. We would like to thank Paweł Naęcz-Jawecki and Julia Kostin for helpful suggestions on the manuscript.

References

- Carl Allen and Timothy Hospedales. Analogies explained: Towards understanding word embeddings. In Kamalika Chaudhuri and Ruslan Salakhutdinov (eds.), *Proceedings of the 36th International Conference on Machine Learning*, volume 97 of *Proceedings of Machine Learning Research*, pp. 223–231. PMLR, 09–15 Jun 2019. URL <https://proceedings.mlr.press/v97/allen19a.html>.
- R.B. Arellano-Valle, J.E. Contreras-Reyes, and M.G. Genton. Shannon entropy and mutual information for multivariate skew-elliptical distributions. *Scandinavian Journal of Statistics*, 49:42–62, 2013.
- Mohamed Ishmael Belghazi, Aristide Baratin, Sai Rajeshwar, Sherjil Ozair, Yoshua Bengio, Aaron Courville, and Devon Hjelm. Mutual information neural estimation. In *International conference on machine learning*, pp. 531–540. PMLR, 2018.
- James Bradbury, Roy Frostig, Peter Hawkins, Matthew James Johnson, Chris Leary, Dougal Maclaurin, George Necula, Adam Paszke, Jake VanderPlas, Skye Wanderman-Milne, and Qiao Zhang. JAX: composable transformations of Python+NumPy programs, 2018. URL <http://github.com/google/jax>.
- David R. Brillinger. Some data analyses using mutual information. *Brazilian Journal of Probability and Statistics*, 18(2):163–182, 2004. ISSN 01030752, 23176199. URL <http://www.jstor.org/stable/43601047>.
- Nick Carrara and Jesse Ernst. Using Monte Carlo tree search to calculate mutual information in high dimensions, 2023.
- Christopher J Cellucci, Alfonso M Albano, and Paul E Rapp. Statistical validation of mutual information calculations: Comparison of alternative numerical algorithms. *Physical review E*, 71(6):066208, 2005.
- Paweł Czyż, Frederic Grabowski, Julia E. Vogt, Niko Beerenwinkel, and Alexander Marx. Beyond normal: On the evaluation of mutual information estimators. In *Thirty-seventh Conference on Neural Information Processing Systems*, 2023.
- Georges A Darbellay and Igor Vajda. Estimation of the information by an adaptive partitioning of the observation space. *IEEE Transactions on Information Theory*, 45(4):1315–1321, 1999.
- Joshua V. Dillon, Ian Langmore, Dustin Tran, Eugene Brevdo, Srinivas Vasudevan, Dave Moore, Brian Patton, Alex Alemi, Matthew D. Hoffman, and Rif A. Saurous. Tensorflow distributions. *CoRR*, abs/1711.10604, 2017. URL <http://arxiv.org/abs/1711.10604>.
- James M. Flegal, Murali Haran, and Galin L. Jones. Markov Chain Monte Carlo: Can we trust the third significant figure? *Statistical Science*, 23(2):250–260, 2008. doi: 10.1214/08-STS257. URL <https://doi.org/10.1214/08-STS257>.
- Sylvia Frühwirth-Schnatter and Gertraud Malsiner-Walli. From here to infinity: sparse finite versus Dirichlet process mixtures in model-based clustering. *Advances in Data Analysis and Classification*, 13(1):33–64, Mar 2019. ISSN 1862-5355. doi: 10.1007/s11634-018-0329-y. URL <https://doi.org/10.1007/s11634-018-0329-y>.
- Weihao Gao, Sreeram Kannan, Sewoong Oh, and Pramod Viswanath. Estimating mutual information for discrete-continuous mixtures. In I. Guyon, U. Von Luxburg, S. Bengio, H. Wallach, R. Fergus, S. Vishwanathan, and R. Garnett (eds.), *Advances in Neural Information Processing Systems*, volume 30. Curran Associates, Inc., 2017. URL https://proceedings.neurips.cc/paper_files/paper/2017/file/ef72d53990bc4805684c9b61fa64a102-Paper.pdf.
- A. Gelman, J.B. Carlin, H.S. Stern, D.B. Dunson, A. Vehtari, and D.B. Rubin. *Bayesian Data Analysis, Third Edition*. Chapman & Hall/CRC Texts in Statistical Science. Taylor & Francis, 2013. ISBN 9781439840955. URL <https://books.google.pl/books?id=ZXL6AQAAQBAJ>.
- Andrew Gelman, Aki Vehtari, Daniel Simpson, Charles C. Margossian, Bob Carpenter, Yuling Yao, Lauren Kennedy, Jonah Gabry, Paul-Christian

-
- Bürkner, and Martin Modrák. Bayesian workflow, 2020.
- Frederic Grabowski, Paweł Czyż, Marek Kočańczyk, and Tomasz Lipniacki. Limits to the rate of information transmission through the MAPK pathway. *Journal of The Royal Society Interface*, 16(152):20180792, 2019. doi: 10.1098/rsif.2018.0792. URL <https://royalsocietypublishing.org/doi/abs/10.1098/rsif.2018.0792>.
- David Haussler and Manfred Opper. Mutual information, metric entropy and cumulative relative entropy risk. *The Annals of Statistics*, 25(6):2451–2492, 1997. doi: 10.1214/aos/1030741081. URL <https://doi.org/10.1214/aos/1030741081>.
- Matthew D. Hoffman and Andrew Gelman. The No-U-Turn Sampler: Adaptively setting path lengths in Hamiltonian Monte Carlo. *Journal of Machine Learning Research*, 15(47):1593–1623, 2014. URL <http://jmlr.org/papers/v15/hoffman14a.html>.
- Marcus Hutter. Distribution of mutual information. In T. Dietterich, S. Becker, and Z. Ghahramani (eds.), *Advances in Neural Information Processing Systems*, volume 14. MIT Press, 2001. URL https://proceedings.neurips.cc/paper_files/paper/2001/file/fb2e203234df6dee15934e448ee88971-Paper.pdf.
- J. P. Imhof. Computing the distribution of quadratic forms in normal variables. *Biometrika*, 48(3/4):419–426, 1961. ISSN 00063444. URL <http://www.jstor.org/stable/2332763>.
- Pavel Izmailov, Sharad Vikram, Matthew D Hoffman, and Andrew Gordon Gordon Wilson. What are Bayesian neural network posteriors really like? In Marina Meila and Tong Zhang (eds.), *Proceedings of the 38th International Conference on Machine Learning*, volume 139 of *Proceedings of Machine Learning Research*, pp. 4629–4640. PMLR, 18–24 Jul 2021. URL <https://proceedings.mlr.press/v139/izmailov21a.html>.
- Takoua Jendoubi and Korbinian Strimmer. A whitening approach to probabilistic canonical correlation analysis for omics data integration. *BMC Bioinformatics*, 20(1):15, Jan 2019. ISSN 1471-2105. doi: 10.1186/s12859-018-2572-9. URL <https://doi.org/10.1186/s12859-018-2572-9>.
- J. Kay. Feature discovery under contextual supervision using mutual information. In *IJCNN International Joint Conference on Neural Networks*, volume 4, pp. 79–84, 1992. doi: 10.1109/IJCNN.1992.227286.
- I. Kobyzev, S. D. Prince, and M. A. Brubaker. Normalizing flows: An introduction and review of current methods. *IEEE Transactions on Pattern Analysis & Machine Intelligence*, 43(11):3964–3979, nov 2021. ISSN 1939-3539. doi: 10.1109/TPAMI.2020.2992934.
- Artemy Kolchinsky and Brendan D. Tracey. Estimating mixture entropy with pairwise distances. *Entropy*, 19(7), 2017. ISSN 1099-4300. doi: 10.3390/e19070361. URL <https://www.mdpi.com/1099-4300/19/7/361>.
- Alexander Kraskov, Harald Stögbauer, and Peter Grassberger. Estimating mutual information. *Physical Review E*, 69(6):066138, 2004.
- J.M. Lee. *Introduction to Smooth Manifolds*. Graduate Texts in Mathematics. Springer, 2nd edition, 2012. ISBN 9781441999825. URL <https://doi.org/10.1007/978-1-4419-9982-5>.
- Sirio Legramanti, Daniele Durante, and David B Dunson. Bayesian cumulative shrinkage for infinite factorizations. *Biometrika*, 107(3):745–752, 05 2020. ISSN 0006-3444. doi: 10.1093/biomet/asaa008. URL <https://doi.org/10.1093/biomet/asaa008>.
- Daniel Lewandowski, Dorota Kurowicka, and Harry Joe. Generating random correlation matrices based on vines and extended onion method. *Journal of Multivariate Analysis*, 100(9):1989–2001, 2009. ISSN 0047-259X. doi: <https://doi.org/10.1016/j.jmva.2009.04.008>. URL <https://www.sciencedirect.com/science/article/pii/S0047259X09000876>.
- Alexander Marx, Lincen Yang, and Matthijs van Leeuwen. Estimating conditional mutual information for discrete-continuous mixtures using multi-dimensional adaptive histograms. In *Proceedings of the SIAM International Conference on Data Mining (SDM)*, pp. 387–395, 2021.
- Nina Miolane, Nicolas Guigui, Alice Le Brigant, Johan Mathe, Benjamin Hou, Yann Thanwerdas, Stefan Heyder, Olivier Peltre, Niklas Koep, Hadi Zaatiti, Hatem Hajri, Yann Cabanes, Thomas Gerald, Paul Chauchat, Christian Shewmake, Daniel Brooks, Bernhard Kainz, Claire Donnat, Susan Holmes, and Xavier Pennec. Geomstats: A Python package for Riemannian geometry in machine learning. *Journal of Machine Learning Research*, 21(223):1–9, 2020. URL <http://jmlr.org/papers/v21/19-027.html>.
- Kevin P. Murphy. *Probabilistic Machine Learning: Advanced Topics*. MIT Press, 2023. URL <http://probml.github.io/book2>.
- Paweł Nałęcz-Jawecki, Paolo Armando Gagliardi, Marek Kočańczyk, Coralie Dessauges, Olivier Pertz, and Tomasz Lipniacki. The MAPK/ERK channel capacity exceeds 6 bit/hour. *PLOS Computational Biology*, 19(5):1–21, 05 2023. doi: 10.1371/

-
- journal.pcbi.1011155. URL <https://doi.org/10.1371/journal.pcbi.1011155>.
- XuanLong Nguyen, Martin J Wainwright, and Michael Jordan. Estimating divergence functionals and the likelihood ratio by penalized convex risk minimization. In J. Platt, D. Koller, Y. Singer, and S. Roweis (eds.), *Advances in Neural Information Processing Systems*, volume 20. Curran Associates, Inc., 2007. URL https://proceedings.neurips.cc/paper_files/paper/2007/file/72da7fd6d1302c0a159f6436d01e9eb0-Paper.pdf.
- Aaron van den Oord, Yazhe Li, and Oriol Vinyals. Representation learning with contrastive predictive coding. *arXiv preprint arXiv:1807.03748*, 2018.
- George Papamakarios, Eric Nalisnick, Danilo Jimenez Rezende, Shakir Mohamed, and Balaji Lakshminarayanan. Normalizing flows for probabilistic modeling and inference. *Journal of Machine Learning Research*, 22(57):1–64, 2021. URL <http://jmlr.org/papers/v22/19-1028.html>.
- K. B. Petersen and M. S. Pedersen. The matrix cookbook, November 2012. URL <http://www2.compute.dtu.dk/pubdb/pubs/3274-full.html>. Version 20121115.
- Du Phan, Neeraj Pradhan, and Martin Jankowiak. Composable effects for flexible and accelerated probabilistic programming in numpyro. *arXiv preprint arXiv:1912.11554*, 2019.
- Juho Piironen and Aki Vehtari. Comparison of Bayesian predictive methods for model selection. *Statistics and Computing*, 27(3):711–735, May 2017. ISSN 1573-1375. doi: 10.1007/s11222-016-9649-y. URL <https://doi.org/10.1007/s11222-016-9649-y>.
- M.S. Pinsker and A. Feinstein. *Information and Information Stability of Random Variables and Processes*. Holden-Day series in time series analysis. Holden-Day, 1964. ISBN 9780816268047.
- Dimitris N Politis. *On the entropy of a mixture distribution*. Purdue University. Department of Statistics, 1991.
- Y. Polyanskiy and Y. Wu. *Information Theory: From Coding to Learning*. Cambridge University Press, 2022. Book draft.
- Tiberiu Popoviciu. Sur les équations algébriques ayant toutes leurs racines réelles. *Mathematica (Cluj)*, 9: 129–145, 1935.
- Kris Sankaran and Susan P. Holmes. Generative models: An interdisciplinary perspective. *Annual Review of Statistics and Its Application*, 10(1):325–352, 2023. doi: 10.1146/annurev-statistics-033121-110134. URL <https://doi.org/10.1146/annurev-statistics-033121-110134>.
- James Watson and Chris Holmes. Approximate Models and Robust Decisions. *Statistical Science*, 31(4): 465 – 489, 2016. doi: 10.1214/16-STS592. URL <https://doi.org/10.1214/16-STS592>.

APPENDIX

A TECHNICAL RESULTS

A.1 Proof of the invariance of the pointwise mutual information profile

Recall a well-known result (Kraskov et al., 2004, Appendix):

Lemma 12 (Invariance of PMI). *Let $X' = f(X)$ and $Y' = g(Y)$, where f and g are diffeomorphisms. Then for every x' and y' we have*

$$\text{PMI}_{X'Y'}(x', y') = \text{PMI}_{XY}(x, y),$$

where $x = f^{-1}(x')$ and $y = g^{-1}(y')$.

Proof. From

$$p_{X'Y'}(x', y') = p_{XY}(x, y) |\det D(f^{-1} \times g^{-1})(x', y')|$$

and analogous quantities we conclude that $p_{X'Y'}$ as well as $p_{X'}$ and $p_{Y'}$ are smooth and everywhere positive functions, so that $\text{PMI}_{X'Y'}$ is well-defined. As $D(f^{-1} \times g^{-1})(x', y')$ is a block matrix with $Df^{-1}(x')$ and $Dg^{-1}(y')$ blocks on the diagonal and other blocks zero, we have $\det D(f^{-1} \times g^{-1})(x', y') = \det Df^{-1}(x') \cdot \det Dg^{-1}(y')$. \square

Now we can prove:

Theorem 3. *Let $P_{XY} \in \mathcal{P}(\mathcal{X}, \mathcal{Y})$ and $f: \mathcal{X} \rightarrow \mathcal{X}$ and $g: \mathcal{Y} \rightarrow \mathcal{Y}$ be diffeomorphisms. Then for $X' = f(X)$ and $Y' = g(Y)$ it holds that $P_{X'Y'} \in \mathcal{P}(\mathcal{X}, \mathcal{Y})$ and $\text{Prof}_{XY} = \text{Prof}_{X'Y'}$.*

Proof. From the proof of Lemma 12 we conclude that $P_{X'Y'} \in \mathcal{P}(\mathcal{X}, \mathcal{Y})$. Then, we note the profile is the pushforward measure

$$\text{Prof}_{XY} := (\text{PMI}_{XY})_{\#} P_{XY}.$$

Now let $B \subseteq \mathbb{R}$ be any set in the Borel σ -algebra and $\mathbf{1}_B$ be its characteristic function. Using the change of variables formula for pushforward measure and invariance of PMI:

$$\begin{aligned} \text{Prof}_{X'Y'}(B) &= \int \mathbf{1}_B(t) d((\text{PMI}_{X'Y'})_{\#} P_{X'Y'})(t) \\ &= \int \mathbf{1}_B(\text{PMI}_{X'Y'}(x', y')) dP_{X'Y'}(x', y') \\ &= \int \mathbf{1}_B(\text{PMI}_{X'Y'}(f(x), g(y))) dP_{XY}(x, y) \\ &= \int \mathbf{1}_B(\text{PMI}_{XY}(x, y)) dP_{XY}(x, y) \\ &= \text{Prof}_{XY}(B) \end{aligned}$$

\square

A.2 Pointwise Mutual Information Profiles

The following result shows that the distributions in all $\mathcal{P}(\mathcal{X}, \mathcal{Y})$ classes with zero mutual information have the same profile:

Proposition 4. *Let X and Y be r.v. with joint distribution $P_{XY} \in \mathcal{P}(\mathcal{X}, \mathcal{Y})$. Then, $\mathbf{I}(X; Y) = 0$ if and only if $\text{Prof}_{XY} = \delta_0$ is the Dirac measure with a single atom at 0.*

Proof. If $\text{Prof}_{XY} = \delta_0$, then the expected value is $\mathbf{I}(X; Y) = 0$. To prove the converse, if $\mathbf{I}(X; Y) = 0$, then X and Y are independent. Hence, $p_{XY}(x, y) = p_X(x)p_Y(y)$ at every point (x, y) and $\text{PMI}_{XY}(x, y) = 0$ everywhere. \square

The following result characterizes the PMI profiles for discrete r.v.:

Proposition 5. *If X and Y are discrete r.v. with $P_{XY} \in \mathcal{P}(\mathcal{X}, \mathcal{Y})$, then the PMI profile is discrete:*

$$\text{Prof}_{XY} = \sum_{x \in \mathcal{X}} \sum_{y \in \mathcal{Y}} p_{XY}(x, y) \delta_{\text{PMI}_{XY}(x, y)}.$$

Proof. The measure P_{XY} is discrete and given by

$$P_{XY} = \sum_{x \in \mathcal{X}} \sum_{y \in \mathcal{Y}} p_{XY}(x, y) \delta_{(x, y)},$$

so its pushforward by the PMI_{XY} function has the form

$$\text{Prof}_{XY} = (\text{PMI}_{XY})_{\#} P_{XY} = \sum_{x \in \mathcal{X}} \sum_{y \in \mathcal{Y}} p_{XY}(x, y) \delta_{\text{PMI}_{XY}(x, y)}.$$

□

Theorem 6. *Let X and Y be r.v. such that the joint distribution $P_{XY} \in \mathcal{P}(\mathbb{R}^m, \mathbb{R}^n)$ is multivariate normal. If $k = \min(m, n)$ and $\rho_1, \rho_2, \dots, \rho_k$ are canonical correlations (Jendoubi & Strimmer, 2019) between X and Y , then the profile Prof_{XY} is a generalized χ^2 distribution, namely the distribution of the variable*

$$T = \mathbf{I}(X; Y) + \sum_{i=1}^k \frac{\rho_i}{2} (Q_i - Q'_i),$$

where Q_i and Q'_i are i.i.d. variables sampled according to the χ_1^2 distribution. In particular, Prof_{XY} is symmetric around its median, which coincides with the mean $\mathbf{I}(X; Y) = -\frac{1}{2} \sum_{i=1}^k \log(1 - \rho_i^2)$, and all the moments of this distribution exist; its variance is equal to $\rho_1^2 + \dots + \rho_k^2$.

Proof. Without loss of generality assume that $m \leq n$. As the PMI profile is invariant to diffeomorphisms (Theorem 3), we can also assume that variables X and Y have been whitened by applying canonical correlation analysis (Jendoubi & Strimmer, 2019), that is $\mathbb{E}[X] = 0$, $\mathbb{E}[Y] = 0$ and the covariance matrix is given by

$$\Sigma = \begin{pmatrix} I_m & \Sigma_{XY} \\ \Sigma_{XY}^T & I_n \end{pmatrix} = \begin{pmatrix} I_m & R & 0 \\ R & I_m & 0 \\ 0 & 0 & I_{n-m} \end{pmatrix}$$

where

$$\Sigma_{XY} = \begin{pmatrix} R & 0_{m \times (n-m)} \end{pmatrix}$$

is an $m \times n$ matrix with the last $n - m$ columns being zero vectors and $R = \text{diag}(\rho_1, \dots, \rho_m)$ being the $m \times m$ diagonal matrix representing canonical correlations.

We will write the inverse in the block form

$$\Sigma^{-1} = \begin{pmatrix} \Lambda_X & \Lambda_{XY} \\ \Lambda_{XY}^T & \Lambda_Y \end{pmatrix} = \begin{pmatrix} \Lambda_X & \tilde{R} & 0 \\ \tilde{R} & \Lambda_X & 0 \\ 0 & 0 & I_{n-m} \end{pmatrix}$$

where the blocks have been calculated using the formula from Petersen & Pedersen (2012, Sec. 9.1):

$$\begin{aligned} \Lambda_X &= (I_m - \Sigma_{XY} \Sigma_{XY}^T)^{-1} = \text{diag}(u_1, \dots, u_m) \\ \Lambda_Y &= (I_n - \Sigma_{XY}^T \Sigma_{XY}) = \text{diag}(u_1, \dots, u_m, 1, \dots, 1) \\ \Lambda_{XY} &= -\Sigma_{XY} \Lambda_Y = \begin{pmatrix} \tilde{R} & 0_{m \times (n-m)} \end{pmatrix}, \end{aligned}$$

where $\tilde{R} = -\text{diag}(u_1 \rho_1, \dots, u_m \rho_m)$ and $u_i = 1 / (1 - \rho_i^2)$.

We define a quadratic form

$$\begin{aligned} s(x, y) &= x^T \Lambda_X x + y^T \Lambda_Y y + 2x^T \Lambda_{XY} y \\ &= \sum_{i=1}^m u_i (x_i^2 + y_i^2 - 2\rho_i x_i y_i) + \sum_{j=m+1}^n y_j^2 \end{aligned}$$

which can be used to calculate log-PDFs:

$$\begin{aligned} \log p_{XY}(x, y) &= -\frac{1}{2} s(x, y) - \frac{1}{2} \log \det \Sigma - \frac{m+n}{2} \log 2\pi, \\ \log p_X(x) &= -\frac{1}{2} x^T x - \frac{m}{2} \log 2\pi, \\ \log p_Y(y) &= -\frac{1}{2} y^T y - \frac{n}{2} \log 2\pi. \end{aligned}$$

Hence,

$$\text{PMI}_{XY}(x, y) = \frac{x^T x + y^T y - s(x, y)}{2} - \frac{1}{2} \log \det \Sigma.$$

We recognize the last summand as

$$\mathbf{I}(X; Y) = \frac{1}{2} \log \left(\frac{\det I_m \cdot \det I_n}{\det \Sigma} \right) = -\frac{1}{2} \log \det \Sigma.$$

Define quadratic form

$$\begin{aligned} q(x, y) &= 2(\text{PMI}_{XY}(x, y) - \mathbf{I}(X; Y)) = x^T x + y^T y - s(x, y) \\ &= \sum_{i=1}^m \left((1 - u_i) (x_i^2 + y_i^2) + 2\rho_i u_i x_i y_i \right), \end{aligned}$$

which has a corresponding matrix

$$Q = \begin{pmatrix} K & F & 0 \\ F & K & 0 \\ 0 & 0 & 0 \end{pmatrix},$$

where

$$K = \text{diag}(1 - u_1, \dots, 1 - u_m)$$

and

$$F = \text{diag}(\rho_1 u_1, \dots, \rho_m u_m).$$

We are interested in the distribution of

$$q(X, Y) = \begin{pmatrix} X^T & Y^T \end{pmatrix} Q \begin{pmatrix} X \\ Y \end{pmatrix},$$

where $(X, Y) \sim \mathcal{N}(0, \Sigma)$.

[Imhof \(1961\)](#) presents a general approach to evaluating the distributions of such quadratic forms. Consider a r.v.

$$Z = \begin{pmatrix} \eta \\ \epsilon \\ \xi \end{pmatrix} \sim \mathcal{N}(0, I_{m+n})$$

which is split into blocks of sizes m , m and $n - m$. We will construct a linear transformation A such that

$$\begin{pmatrix} X \\ Y \end{pmatrix} = A \begin{pmatrix} \eta \\ \epsilon \\ \xi \end{pmatrix}.$$

Then, the distribution of $q(X, Y)$ is the distribution of

$$Z^T A^T Q A Z, \quad Z \sim \mathcal{N}(0, I_{m+n}).$$

We will construct A as

$$A = \begin{pmatrix} P_- & P_+ & 0 \\ -P_- & P_+ & 0 \\ 0 & 0 & I_{n-m} \end{pmatrix}$$

where

$$P_- = \text{diag} \left(\sqrt{\frac{1-\rho_1}{2}}, \dots, \sqrt{\frac{1-\rho_m}{2}} \right), \quad P_+ = \text{diag} \left(\sqrt{\frac{1+\rho_1}{2}}, \dots, \sqrt{\frac{1+\rho_m}{2}} \right).$$

We calculate

$$A A^T = \begin{pmatrix} P_-^2 + P_+^2 & P_+^2 - P_-^2 & 0 \\ P_+^2 - P_-^2 & P_-^2 + P_+^2 & 0 \\ 0 & 0 & I_{n-m} \end{pmatrix} = \begin{pmatrix} I_m & R & 0 \\ R & I_m & 0 \\ 0 & 0 & I_{n-m} \end{pmatrix} = \Sigma$$

and

$$A^T Q A = \begin{pmatrix} 2P_-^2(K-F) & 0 & 0 \\ 0 & 2P_+^2(K+F) & 0 \\ 0 & 0 & 0 \end{pmatrix},$$

where

$$2P_-^2(K-F) = \text{diag}(-\rho_1, \dots, -\rho_m), \quad 2P_+^2(K+F) = \text{diag}(\rho_1, \dots, \rho_m).$$

Hence, the distribution of $q(X, Y)$ is the same as the distribution of

$$\sum_{i=1}^m \rho_i (-\eta_i^2 + \epsilon_i^2) + \sum_{j=1}^{n-m} 0 \cdot \xi_j^2,$$

where $(\eta, \epsilon, \xi) \sim \mathcal{N}(0, I_{m+n})$. To summarize, let $Q_1, \dots, Q_m, Q'_1, \dots, Q'_m$ be i.i.d. random variables distributed according to the χ_1^2 distribution. The quadratic form $q(X, Y)$ has the distribution the same as

$$\sum_{i=1}^m \rho_i (Q_i - Q'_i),$$

which can also be written as

$$q(X, Y) \sim \sum_{i=1}^m (\rho_i \chi_1^2 - \rho_i \chi_1^2).$$

Note that this distribution is symmetric around 0. We can now reconstruct the profile from $q(X, Y)$:

$$\text{Prof}_{XY} = \mathbf{I}(X; Y) + \sum_{i=1}^m \left(\frac{\rho_i}{2} \chi_1^2 - \frac{\rho_i}{2} \chi_1^2 \right),$$

which is symmetric around $\mathbf{I}(X; Y)$ and, in agreement with Proposition 4, degenerates to the atomic distribution δ_0 if and only if $\mathbf{I}(X; Y) = 0$, which is equivalent to $\rho_i = 0$ for all i .

As a linear combination of independent χ_1^2 variables, profile has all finite moments. Using the fact that the variance of χ_1^2 distribution is 2, and quadratic scaling of variance, each term has variance $2 \cdot (\rho_i/2)^2 = \rho_i^2/2$. As variances of independent variables are additive, we can sum up all the $2m$ terms to obtain $\rho_1^2 + \dots + \rho_m^2$. \square

Proposition 13. *With fixed mutual information, the variance of the PMI profile is maximized when $\rho_1^2 = \rho_2^2 = \dots = \rho_m^2$.*

Proof. Let $a_i = 1 - \rho_i^2$. To maximize the variance we equivalently have to minimize $a_1 + \dots + a_m$ preserving given constraint on mutual information and $a_i \in (0, 1]$.

The constraint on mutual information takes the form

$$\mathbf{I}(X; Y) = -\frac{1}{2} \sum_{i=1}^m \log(1 - \rho_i^2) = -\frac{1}{2} \log(a_1 \cdots a_m).$$

Hence, the product $a_1 \cdots a_m$ has to be constant. Denote this constant by A^m for $A \in (0, 1]$ as well.

Let a_1, \dots, a_m be any minimum of $a_1 + \dots + a_m$ under the constraints $a_1 \cdots a_m = A^m$ and $a_i \in (0, 1]$. From the inequality between arithmetic and geometric means we note that

$$\frac{a_1 + \dots + a_m}{m} \geq \sqrt[m]{a_1 \cdots a_m} = A,$$

where the equality holds only if $a_1 = \dots = a_m = A$. Hence, this is the unique minimum under constraints provided. It follows that $\rho_1^2 = \dots = \rho_m^2$. Writing ρ^2 for the common value, we have

$$\rho^2 = 1 - \exp(-2\mathbf{I}(X; Y)/m)$$

and

$$V = m\rho^2 = m(1 - \exp(-2\mathbf{I}(X; Y)/m)).$$

The mutual information can also be written as function of variance

$$\mathbf{I}(X; Y) = -\frac{1}{2}m \log(1 - \rho^2) = -\frac{1}{2}m \log(1 - V/m).$$

□

Proposition 14. *With fixed non-zero mutual information the variance of the PMI profile is minimized when $\rho_i \neq 0$ for exactly one i .*

Proof. Let $a_i \in (0, 1]$ be any numbers. We have

$$(1 - a_1)(1 - a_2) \geq 0$$

which is equivalent to

$$1 + a_1 a_2 \geq a_1 + a_2$$

where the equality holds if and only if $a_1 = 1$ or $a_2 = 1$.

Using the principle of mathematical induction one can prove a more general inequality:

$$\begin{aligned} a_1 a_2 \cdots a_m + (m - 1) &= 1 + a_1(a_2 \cdots a_m) + (m - 2) \\ &\geq a_1 + (a_2 \cdots a_m + (m - 2)) \\ &\geq a_1 + a_2 + (a_3 \cdots a_m + (m - 3)) \\ &\vdots \\ &\geq a_1 + a_2 + \cdots + a_m. \end{aligned}$$

Let us analyze when the equality can hold. To obtain equality in the first step, we need $a_1 = 1$ or $a_2 \cdots a_m = 1$, which, given the constraints $a_i \in (0, 1]$ would mean that $a_2 = \dots = a_m = 1$. Reasoning inductively, one proves that equality holds only when at least $m - 1$ among these numbers are 1.

Let us apply the above reasoning to the numbers $a_i = 1 - \rho_i^2$ and note that we are solving a maximization problem $a_i \in (0, 1]$ under a constraint

$$a_1 \cdots a_m = P.$$

Using the argument above we note that all the maxima for the above problem are permutations of the sequence $P, 1, 1, \dots, 1$. This proves that at most one $\rho_i^2 \neq 0$, what it turns results in at most one $\rho_i \neq 0$. □

A.3 Proof of the failing channel inequality

In this section we prove:

Proposition 11. *Consider variables X , Y and Y' , such that*

$$p_{XY'}(x, y) = (1 - \alpha)p_{XY}(x, y) + \alpha n(y)p_X(x)$$

with contamination level $\alpha \in [0, 1]$. Then,

$$\mathbf{I}(X; Y') \leq (1 - \alpha)\mathbf{I}(X; Y).$$

Proof. Let $Z \sim \text{Bernoulli}(1 - \alpha)$ be an auxiliary variable. We have $(X, Y') \mid Z = 1 \sim P_{XY}$ and $(X, Y') \mid Z = 0 \sim P_X \otimes N_Y$.

From the data processing inequality and chain rule we conclude that

$$\mathbf{I}(X; Y') \leq \mathbf{I}(X; Y', Z) = \mathbf{I}(X; Z) + \mathbf{I}(X; Y' \mid Z).$$

Now note that X and Z are independent, so $\mathbf{I}(X; Z) = 0$.

Hence,

$$\begin{aligned} \mathbf{I}(X; Y') &\leq \mathbf{I}(X; Y' \mid Z) \\ &= \alpha \mathbf{D}_{\text{KL}}(P_{XY' \mid Z=0} \parallel P_{X \mid Z=0} \otimes P_{Y' \mid Z=0}) + (1 - \alpha) \mathbf{D}_{\text{KL}}(P_{XY' \mid Z=1} \parallel P_{X \mid Z=1} \otimes P_{Y' \mid Z=1}) \\ &= \alpha \mathbf{D}_{\text{KL}}(P_{XY' \mid Z=0} \parallel P_X \otimes N_Y) + (1 - \alpha) \mathbf{D}_{\text{KL}}(P_{XY} \parallel P_X \otimes P_Y) \\ &= \alpha \mathbf{D}_{\text{KL}}(P_X \otimes N_Y \parallel P_X \otimes N_Y) + (1 - \alpha) \mathbf{I}(X; Y) \\ &= (1 - \alpha) \mathbf{I}(X; Y). \end{aligned}$$

□

A.4 Constructing new fine distributions

In this section we prove Proposition 8 and Proposition 9.

Proposition 8. *If P_{XY} is fine and f and g are diffeomorphisms with tractable Jacobians, then $P_{f(X)g(Y)}$ is fine.*

Proof. From the proof of Lemma 12 and the assumption of tractability of the Jacobians of f and g we obtain the tractability of the formulae for the densities $p_{f(X)g(Y)}$, $p_{f(X)}$ and $p_{g(Y)}$. Sampling $(f(X), g(Y))$ amounts to sampling (X, Y) and then transforming the sample using f and g . □

Proposition 9. *Consider a mixture distribution $P_{X'Y'}$ with weights w_1, \dots, w_K and component distributions $P_{X_1Y_1}, \dots, P_{X_KY_K}$. If all component distributions are fine, then also the mixture distribution is fine.*

Proof. We can evaluate the densities $p_{X'Y'}(x, y)$, $p_{X'}(x)$ and $p_{Y'}(y)$ of the mixture distribution using the weighted sums of $p_{X_kY_k}(x, y)$, $p_{X_k}(x)$ and $p_{Y_k}(y)$, respectively. To sample $(X', Y') \sim P_{X'Y'}$ from the mixture distribution we can sample an auxiliary variable $Z \sim \text{Categorical}(K; w_1, \dots, w_K)$. Then, we have $((X', Y') \mid Z = k) = (X_k, Y_k)$, so that we can sample from $P_{X_kY_k}$. □

A.5 Approximation with smooth densities

In this section, we prove the following result:

Theorem 15. *Let X and Y be random variables with joint distribution P_{XY} and finite mutual information $\mathbf{I}(X; Y) < \infty$. Then, there exists a sequence of random variables (X_k, Y_k) for $k = 1, 2, \dots$ such that:*

1. Each $P_{X_kY_k} \in \mathcal{P}(m, n)$.
2. Distributions $P_{X_kY_k}$ weakly converge to P_{XY} as $k \rightarrow \infty$.

3. *Mutual information is preserved:*

$$\lim_{k \rightarrow \infty} \mathbf{I}(X_k; Y_k) = \mathbf{I}(X; Y).$$

The proof will automatically follow from two lemmata.

Lemma 16. *Let X be a random variable on \mathbb{R}^k . Let N be a r.v. independent of X distributed according to the multivariate normal distribution $\mathcal{N}(0, \sigma^2 I)$ with $\sigma > 0$. Then the distribution of $X + N$ has a PDF which is everywhere smooth and positive.*

Proof. Let P_X be the distribution of X and f be the PDF of the multivariate normal distribution $\mathcal{N}(0, \sigma^2 I)$, which is bounded, smooth, and everywhere positive. The convolution of P_X and normal density has a PDF

$$(f * P_X)(x) = \int f(x - y) dP_X(y) = \mathbb{E}[f(x - X)].$$

From the dominated convergence theorem it follows that all the partial derivatives of $\partial_j(f * P_X)$ exist and are given by $(\partial_j f) * P_X$. From the principle of mathematical induction we conclude that $f * P_X$ is smooth.

Positivity follows from the fact that the random variable $f(x - X)$ is strictly positive, so that its expected value is strictly positive as well. \square

The second lemma is the following:

Lemma 17. *Assume that $\mathbf{I}(X; Y) < \infty$. Let $X_k = X + N_k$ and $Y_k = Y + M_k$ where N_k and M_k are independent noise variables distributed according to $\mathcal{N}(0, k^{-2} I)$. Then*

$$\lim_{k \rightarrow \infty} \mathbf{I}(X_k; Y_k) = \mathbf{I}(X; Y).$$

Proof. Observe that for every k the equality $\mathbf{I}(X_k; Y_k) \leq \mathbf{I}(X; Y)$ holds. This is a simple corollary of the data processing inequality applied to the variables (X_k, N_k) and (Y_k, M_k) . Then, note that $P_{X_k Y_k}$ converges weakly to P_{XY} . As mutual information is assumed to be finite, it is given by the Kullback–Leibler divergence, which is lower semicontinuous. This proves the reverse inequality. \square

A.6 Creating and destroying information with mixtures

Let $A = (0, 1)$ and $B = (1, 2)$ be two disjoint intervals of unit length. We define two pairs of random variables:

$$(X_1, Y_1) \sim \text{Uniform}(A \times A), \quad (X_2, Y_2) \sim \text{Uniform}(B \times B).$$

Note that

$$\mathbf{I}(X_1; Y_1) = \mathbf{I}(X_2; Y_2) = 0.$$

If $(X, Y) \sim 0.5P_{X_1 Y_1} + 0.5P_{X_2 Y_2}$ is distributed according to a mixture, we have

$$p_{XY}(x, y) = \frac{1}{2} \mathbf{1}[(x, y) \in A \times A \cup B \times B]$$

and

$$p_X(x) = \frac{1}{2} \mathbf{1}[x \in A \cup B], \quad p_Y(y) = \frac{1}{2} \mathbf{1}[y \in A \cup B].$$

Hence,

$$\text{PMI}_{XY}(x, y) = \log 2 \cdot \mathbf{1}[(x, y) \in A \times A \cup B \times B]$$

and

$$\mathbf{I}(X; Y) = \frac{1}{2} \log 2 + \frac{1}{2} \log 2 = \log 2.$$

For a second example, demonstrating vanishing mutual information, recall the distribution constructed as above:

$$p_{XY}(x, y) = \frac{1}{2} \mathbf{1}[(x, y) \in A \times A \cup B \times B]$$

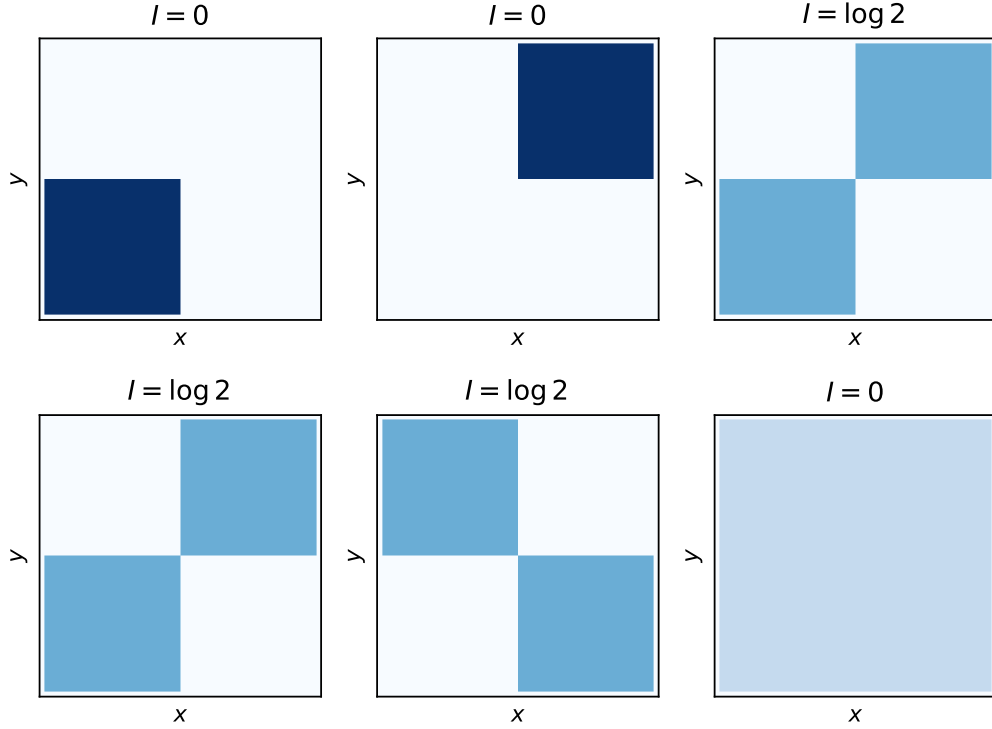


Figure 7: Top row: two distributions with zero MI can be mixed to obtain a distribution with non-zero MI. Bottom row: two distributions with non-zero MI can be mixed to obtain a distribution with zero MI.

and a symmetric one

$$p_{UV}(x, y) = \frac{1}{2} \mathbf{1}[(x, y) \in A \times B \cup B \times A].$$

We have

$$\mathbf{I}(X; Y) = \mathbf{I}(U; V) = \log 2.$$

On the other hand, the mixture distribution

$$(Z, T) \sim 0.5P_{XY} + 0.5P_{UV}$$

has zero mutual information, $\mathbf{I}(Z; T) = 0$, as

$$\begin{aligned} p_{ZT}(x, y) &= \frac{1}{4} \mathbf{1}[(x, y) \in (A \cup B) \times (A \cup B)] \\ &= \frac{1}{2} \mathbf{1}[x \in A \cup B] \cdot \frac{1}{2} \mathbf{1}[y \in A \cup B] \\ &= p_Z(x) \cdot p_T(y). \end{aligned}$$

Note that similar examples can be constructed in the fine distribution family by using mixtures of multivariate normal distributions.

This demonstrates that mixtures can create and destroy information. There is however an upper bound on the amount of information mixtures can create (see [Haussler & Opper \(1997\)](#) and [Kolchinsky & Tracey \(2017\)](#)):

Proposition 10. Consider r.v. (X_k, Y_k) such that $\mathbf{I}(X_k; Y_k) < \infty$ for $k = 1, \dots, K$ and their mixture (X', Y') with weights w_1, \dots, w_K . The following inequalities apply:

$$0 \leq \mathbf{I}(X'; Y') \leq \log K + \sum_{k=1}^K w_k \mathbf{I}(X_k; Y_k).$$

Moreover, these inequalities are tight:

1. There exists a mixture such that $\mathbf{I}(X'; Y') = \log K$ even though $\mathbf{I}(X_k; Y_k) = 0$ for all k .
2. There exists a mixture such that $\mathbf{I}(X'; Y') = 0$ even though $\mathbf{I}(X_k; Y_k) > 0$ for all k .

Proof. The examples provide explicit constructions of distributions with the specified properties. To prove the upper bound, consider a variable $Z \sim \text{Categorical}(K; w_1, \dots, w_K)$. The random variables corresponding to the mixture distribution, (X', Y') , have conditional distributions

$$(X', Y') \mid Z = k \sim P_{X_k Y_k}.$$

From the data processing inequality and chain rule we have

$$\mathbf{I}(X'; Y') \leq \mathbf{I}(X'; Y', Z) = \mathbf{I}(X'; Z) + \mathbf{I}(X'; Y' \mid Z).$$

As Z is discrete, the first summand, $\mathbf{I}(X'; Z)$, is bounded from above by the entropy $H(Z)$ (Polyanskiy & Wu, 2022, Th. 3.4(e)), which cannot exceed $\log K$ (Polyanskiy & Wu, 2022, Th. 1.4(b)). The second summand can be written as

$$\begin{aligned} \mathbf{I}(X'; Y' \mid Z) &= \sum_{k=1}^K P(Z = k) \mathbf{D}_{\text{KL}}(P_{X'Y'|Z=k} \parallel P_{X'|Z=k} \otimes P_{Y'|Z=k}) \\ &= \sum_{k=1}^K w_k \mathbf{D}_{\text{KL}}(P_{X_k Y_k} \parallel P_{X_k} \otimes P_{Y_k}) = \sum_{k=1}^K w_k \mathbf{I}(X_k; Y_k). \end{aligned}$$

□

B DISTRIBUTIONS INVOLVING DISCRETE VARIABLES

The formalism in Section 2 is applicable to both continuous and discrete random variables, although in Section 3.1 we focus on the distributions in which both X and Y are continuous. If X and Y are discrete, mutual information $\mathbf{I}(X; Y)$ can be calculated analytically from the joint probability matrix and there exist numerous approaches to estimate it from collected samples (Hutter, 2001; Brillinger, 2004).

In this section we consider the mixed case, in which one variable is continuous and the other one is discrete. For example, Carrara & Ernst (2023) describe a particle physics experiment in which X is an 18-dimensional random variable, but Y is binary. Grabowski et al. (2019) consider a cell transmitting information through the MAPK signalling pathway, assuming the input signal X to be discrete and the measured response Y to be continuous.

Yet, there are only a few distributions P_{XY} with known ground-truth mutual information assuming this discrete-continuous case. Gao et al. (2017, Sec. 5) describe a discrete random variable X which is uniformly sampled from the set $\mathcal{X} = \{0, \dots, m-1\}$ and the continuous Y variable is sampled as

$$(Y \mid X = x) \sim \text{Uniform}(x, x + 2),$$

which is therefore distributed on $\mathcal{Y} = (0, m + 1)$. Gao et al. (2017) prove that mutual information in this case is

$$\mathbf{I}(X; Y) = \log m - \frac{m}{m-1} \log 2$$

for $m \geq 2$ and $\mathbf{I}(X; Y) = 0$ for $m = 1$ and consider a multivariate analogue of this distribution, in which pairs of variables (X_k, Y_k) for $k = 1, \dots, K$ are sampled independently using the above procedure. Then, they are concatenated into multivariate vectors (X_1, \dots, X_K) and (Y_1, \dots, Y_K) with K times larger mutual information.

We will show how to relate the bivariate example to the framework of fine (multivariate case can be constructed analogously). Note that the joint distribution P_{XY} is not strictly in $\mathcal{P}(\mathcal{X}, \mathcal{Y})$, as it is supported on the one-dimensional manifold $\mathcal{M} \subset \mathcal{X} \times \mathcal{Y}$ with m connected components (cf. Politis (1991) and Marx et al. (2021)), on which

$$p_{XY}(x, y) = \frac{1}{2m} \mathbf{1}[y \in (x, x + 2)],$$

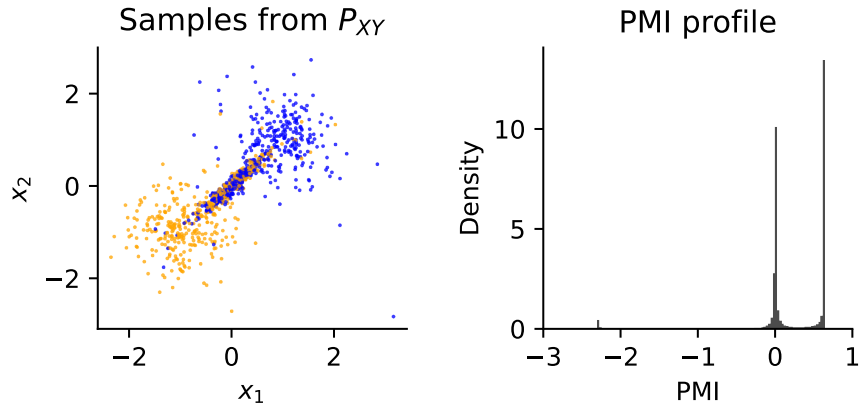


Figure 8: Left: samples from the P_{XY} distribution, colored by the value of the binary variable Y . Right: the PMI profile of P_{XY} distribution.

but it is possible to extend the definitions of Section 2, so that this technical difficulty is resolved. The marginal distributions are tractable and admit PDFs:

$$p_X(x) = 1/m,$$

$$p_Y(y) = \sum_{x=0}^{m-1} p_{XY}(x, y).$$

Although p_Y is not smooth on \mathcal{Y} (at integer points), this technical difficulty can also be resolved as this set is of measure zero. Hence, although this distribution is not strictly fine, it can still be modelled using the introduced framework.

Next, Gao et al. (2017, Sec. 5) consider the zero-inflated Poissonization of the exponential random variable valued in $\mathcal{X} = \{x \in \mathbb{R} \mid x \geq 0\}$, with: $X \sim \text{Exp}(1)$ and Y being a discrete random variable valued in the set of non-negative integers $\mathcal{Y} = \{0, 1, 2, \dots\}$:

$$(Y \mid X = x) \sim p \delta_0 + (1 - p) \text{Poisson}(x).$$

They show that

$$\mathbf{I}(X; Y) = (1 - p) \left(2 \log 2 - \gamma - \sum_{k=0}^{\infty} \log k \cdot 2^{-k} \right),$$

where γ is the Euler–Mascheroni constant.

To use fine distributions in this case, one has to formally extend the definition of $\mathcal{P}(\mathcal{X}, \mathcal{Y})$ as \mathcal{X} is a manifold with boundary (Lee, 2012, Ch. 1). The joint probability distribution is then given by

$$p_{XY}(x, y) = p_X(x) \cdot p_{Y|X}(y \mid x) = e^{-x} \cdot \left(p \cdot \mathbf{1}[y = 0] + (1 - p) \frac{e^{-x} x^y}{y!} \right)$$

and the PMF function of the Y variable is also analytically known:

$$p_Y(y) = p \cdot \mathbf{1}[y = 0] + (1 - p) \cdot 2^{-(1+y)}$$

Hence, the framework of fine distributions, with minor modifications, can accommodate the above distributions.

However, it also allows one to create more expressive distributions, for which analytical formulae for ground-truth mutual information are not available, but can be approximated with the Monte Carlo methods as explained in Section 2: consider a continuous random variable X and a discrete random variable Y . To introduce a dependency between X and Y variable, we can use a mixture of distributions in which the component variables

are independent, i.e., $P_{X_k Y_k} = P_{X_k} \otimes P_{Y_k}$. Therefore, we consider a graphical model $X \leftarrow Z \rightarrow Y$, in which the distributions $P_{X_k} = P_{X|Z=k}$ are known and have tractable PDFs. The distributions of $P_{Y_k} = P_{Y|Z_k}$ are given by probability tables. Monte Carlo estimators of Section 2 can then be used to estimate $\mathbf{I}(X; Y)$ with high accuracy. Note also that this general procedure includes the case $X \leftarrow Y$ by setting $Z = Y$.

We illustrate it in a simple example with $\mathcal{X} = \mathbb{R}^2$, $\mathcal{Y} = \{0, 1\}$ and $K = 3$ components.

The first component will model a cluster in the \mathcal{X} space, strongly associated with $Y = 1$ value. For P_{X_1} we use a bivariate Student distribution centered at $(1, 1)$ with isotropic dispersion $\Omega = 0.2 \cdot I_2$ and 8 degrees of freedom. We take P_{Y_1} to be the Bernoulli variable with probability $P(Y_1 = 1) = 0.95$.

Analogously, we define a second cluster, strongly associated with $Y = 0$ value: P_{X_2} is a bivariate Student distribution with the same dispersion matrix, but centered at $(-1, -1)$ and with 8 degrees of freedom. Then, Y_2 is a Bernoulli variable with $P(Y_2 = 1) = 0.05$.

We then define a third component using a bivariate normal distribution centered at $(0, 0)$ and with covariance matrix

$$\Sigma = 0.1 \begin{pmatrix} 1 & 0.95 \\ 0.95 & 1 \end{pmatrix}.$$

This component is not informative of Y , that is $P(Y_3 = 1) = 0.5$.

We used weights $w_1 = w_2 = 1/4$ and $w_3 = 1/2$, what resulted in the distribution visualised in Fig. 8. We estimated both the profile and the mutual information using $N = 10^6$ samples and obtained $\mathbf{I}(X; Y) = 0.224$ with MCSE of $5.1 \cdot 10^{-4}$.

In principle, the above construction can be used to generate realistic high-dimensional data sets (e.g., audio or image) with known ground-truth mutual information, by assuming the generative model $Y \rightarrow X$ (i.e., $Z = Y$) and modelling each P_{X_k} using a normalizing flow or an autoregressive model (Murphy, 2023, Ch. 22) trained on an auxiliary data set with fixed label $Y_k = y_k$. Hence, at least in principle, one could obtain highly-expressive generative process $p_{X|Y}(x | y)$ with tractable probability and sampling. Pairing this with an arbitrary probability vector $p_Y(y)$ one can obtain $p_{XY}(x, y)$ and $p_X(x)$ even for high-dimensional data sets, so that Monte Carlo estimator can be used to determine the ground-truth mutual information. However, we anticipate possible practical difficulties with scaling up the proposed approach to high-dimensional data and we leave empirical investigation of this topic to future work.

C EXPERIMENTAL DETAILS

C.1 New distributions

We constructed the X distribution as a mixture of bivariate normal distributions with equal weights, zero mean and covariance matrices specified by

$$\Sigma_{\pm} = 0.3 \begin{pmatrix} 1 & \pm 0.9 \\ \pm 0.9 & 1 \end{pmatrix}.$$

Note that the marginal distributions of each of component distributions is $\mathcal{N}(0, 0.3^2)$ and subsequently their mixture has exactly the same marginal distributions. This is therefore an interesting example of a distribution in which the joint probability distribution is not multivariate normal, although the marginal distributions of X and Y variables are normal individually.

The AI distribution was constructed as an equally-weighted mixture of six bivariate normal distributions with

equal weights and the following parameters:

$$\begin{aligned}
\mu_1 &= (1, 0) \\
\Sigma_1 &= \text{diag}(0.01, 0.2) \\
\mu_2 &= (1, 1) \\
\Sigma_2 &= \text{diag}(0.05, 0.001) \\
\mu_3 &= (1, -1) \\
\Sigma_3 &= \text{diag}(0.05, 0.001) \\
\mu_4 &= (-0.8, -0.2) \\
\Sigma_4 &= \text{diag}(0.03, 0.001) \\
\mu_5 &= (-1.2, 0) \\
\Sigma_5 &= \begin{pmatrix} 0.04 & 0.085 \\ 0.085 & 0.2 \end{pmatrix} \\
\mu_6 &= (-0.4, 0) \\
\Sigma_6 &= \begin{pmatrix} 0.04 & -0.085 \\ -0.085 & 0.2 \end{pmatrix}
\end{aligned}$$

The **Galaxy** distribution was constructed as an equally-weighted mixture of isotropic multivariate normal distributions with $\mu_{\pm} = \pm(1, 1, 1)$ and unit covariance matrix and the X variable was transformed using the spiral diffeomorphism with $v = 0.5$ (cf. [Czyż et al. \(2023\)](#)).

The **Waves** distribution was created as an equally-weighted mixture of 12 multivariate normal distributions with equal covariance matrices $\Sigma = \text{diag}(0.1, 1, 0.1)$ and mean vectors

$$\mu_i = (x, 0, x \bmod 4), \quad i \in \{0, 1, \dots, 11\}.$$

This construction results in a distribution where different vertical components of the X variable are assigned Y values calculated modulo 4. Then, we transformed the X variable with a continuous injection

$$f(x_1, x_2) = (x_1 + 5 \sin(3x_2), x_2),$$

which does not change the mutual information. Finally, we applied the affine mappings

$$a_1(x) = 0.1x - 0.8, \quad a_2(y) = 0.5y,$$

to make the range of the typical values comparable with other distributions.

To estimate the ground-truth mutual information we used the Monte Carlo approach described in [Section 2](#) with $N = 200\,000$ samples.

C.2 Estimator hyperparameters

[Czyż et al. \(2023, Appendix E.4\)](#) study the effects of hyperparameters on mutual information estimators. We decided to use the histogram-based estimator ([Cellucci et al., 2005](#); [Darbellay & Vajda, 1999](#)) with a fixed number of 10 bins per dimension and the popular KSG estimator ([Kraskov et al., 2004](#)) with $k = 10$ neighbors. Canonical correlation analysis ([Kay, 1992](#); [Brillinger, 2004](#)) does not have any hyperparameters. Finally, we employed neural estimators (InfoNCE ([Oord et al., 2018](#)) and MINE ([Belghazi et al., 2018](#))) with the neural critic being a ReLU network with 16 and 8 hidden neurons, as it obtained competitive performance in the benchmark of [Czyż et al. \(2023, Appendix E.4\)](#).

As a preprocessing strategy, we followed [Czyż et al. \(2023, Appendix E.3\)](#) and transformed all samples to have zero empirical mean and unit variance along each dimension.

D GAUSSIAN MIXTURE MODELS

Recall from [Sec. 4](#) that for Bayesian estimation of mutual information consists of the following steps:

-
1. Propose a parametric generative model of the data, $P_\theta := P(X, Y \mid \theta)$, and assume a prior $P(\theta)$ on the parameter space.
 2. Use a Markov chain Monte Carlo method to obtain a sample $\theta^{(1)}, \dots, \theta^{(m)}$ from the posterior $P(\theta \mid X_1, Y_1, \dots, X_N, Y_N)$.
 3. Estimate mutual information (and the PMI profile) for each $\theta^{(m)}$ using the Monte Carlo method described in Sec. 2.
 4. Validate the findings using e.g., posterior predictive checks and cross-validation.

We consider the following sparse Gaussian mixture model with $K = 10$ components:

$$\begin{aligned}
 \pi &\sim \text{Dirichlet}(K; 1/K, 1/K, \dots, 1/K), \\
 Z_n \mid \pi &\sim \text{Categorical}(\pi), & n = 1, \dots, N, \\
 \mu_k &\sim \mathcal{N}(0, 3^2 I_D), & k = 1, \dots, K, \\
 \Sigma_k &\sim \text{ScaledLKJ}(1, 1), & k = 1, \dots, K, \\
 (X_n, Y_n) \mid Z_n, \{\mu_k, \Sigma_k\} &\sim \mathcal{N}(\mu_{Z_n}, \Sigma_{Z_n}), & n = 1, \dots, N.
 \end{aligned}$$

Sampling a single covariance matrix Σ from ScaledLKJ(σ, η) distribution corresponds to sampling the correlation matrix R from the Lewandowski-Kurowicka-Joe (LKJ) distribution (Lewandowski et al., 2009):

$$p(R) \propto (\det R)^{\eta-1},$$

sampling the scale parameters

$$\lambda_1, \lambda_2, \dots, \lambda_D \sim \text{HalfCauchy}(\text{scale}=\sigma),$$

and then constructing the covariance matrix as $\Sigma_{ij} = R_{ij} \lambda_i \lambda_j$.

The sparse Dirichlet prior is a finite-dimensional alternative to the Dirichlet process, which truncates the number of occupied clusters depending on the data (Frühwirth-Schnatter & Malsiner-Walli, 2019). In particular, the *a priori* expected number of clusters depends on the number of data points to be observed.

To perform Markov chain Monte Carlo sampling, we implemented the model in NumPyro (Phan et al., 2019), with local latent variables Z_n marginalized out and performed sampling using the NUTS sampler (Hoffman & Gelman, 2014). We used 2000 warm-up steps and collected 800 samples.

The m th sample is therefore given by

$$\theta^{(m)} = \left(\pi^{(m)}, \left(\mu_k^{(m)}, \Sigma_k^{(m)} \right)_{k=1, \dots, K} \right)$$

which is then used to parametrize a Gaussian mixture distribution $P_{\theta^{(m)}}$.

Finally, using Monte Carlo method described in Sec. 2 (with 100,000 samples) we then estimated mutual information $\mathbf{I}(P_{\theta^{(m)}})$ and the profile.

We used the above procedure to perform inference in the model applied to the X, AI, Waves and Galaxy distributions, changing the number of data points $N \in \{125, 250, 500, 1000\}$. We visualise the observed sample, a single posterior predictive sample and posterior on mutual information and the PMI profile in Fig. 9, Fig. 10, Fig. 11 and Fig. 12.

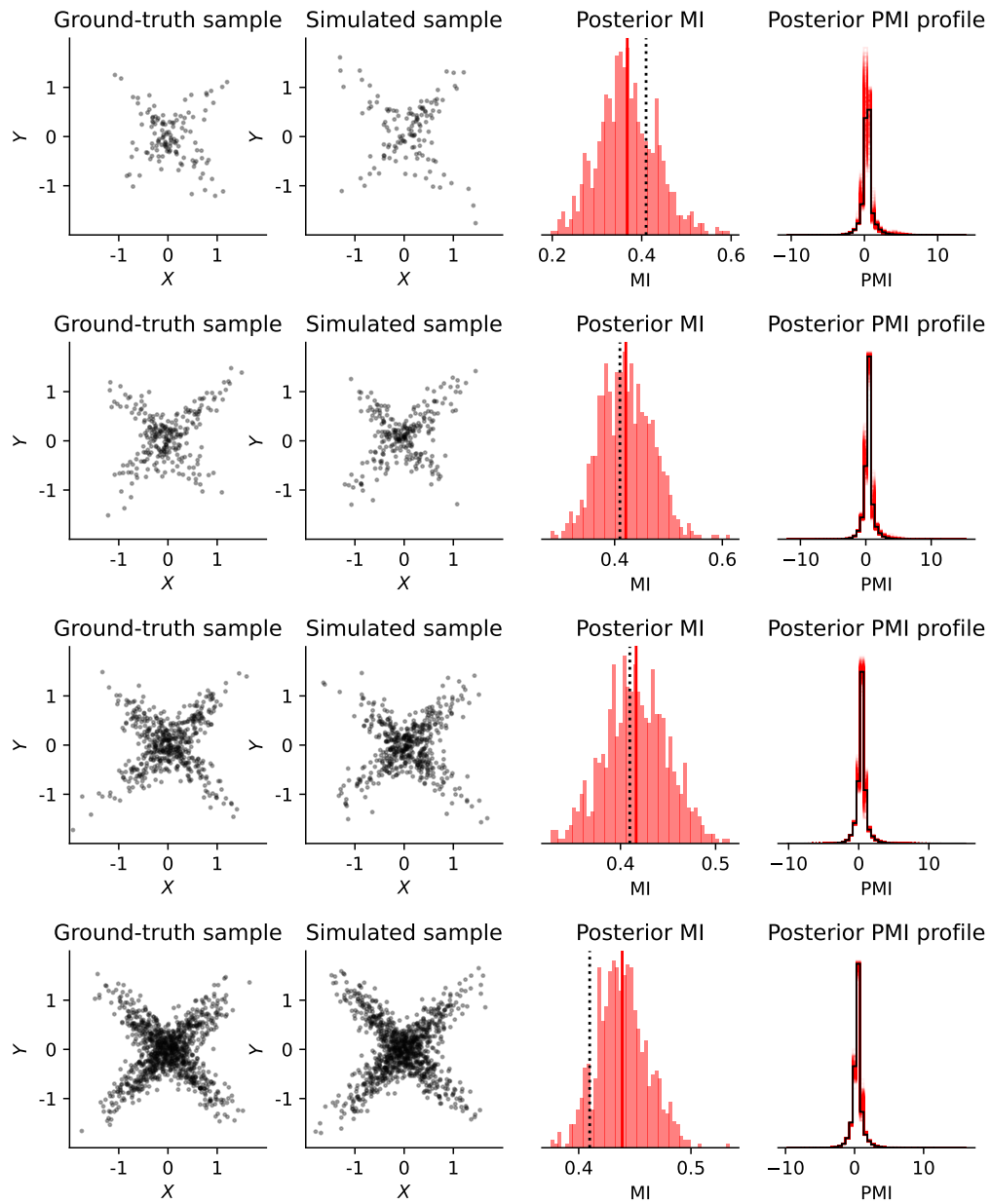


Figure 9: Gaussian mixture model fitted to the X distribution with 125, 250, 500 and 1000 samples.

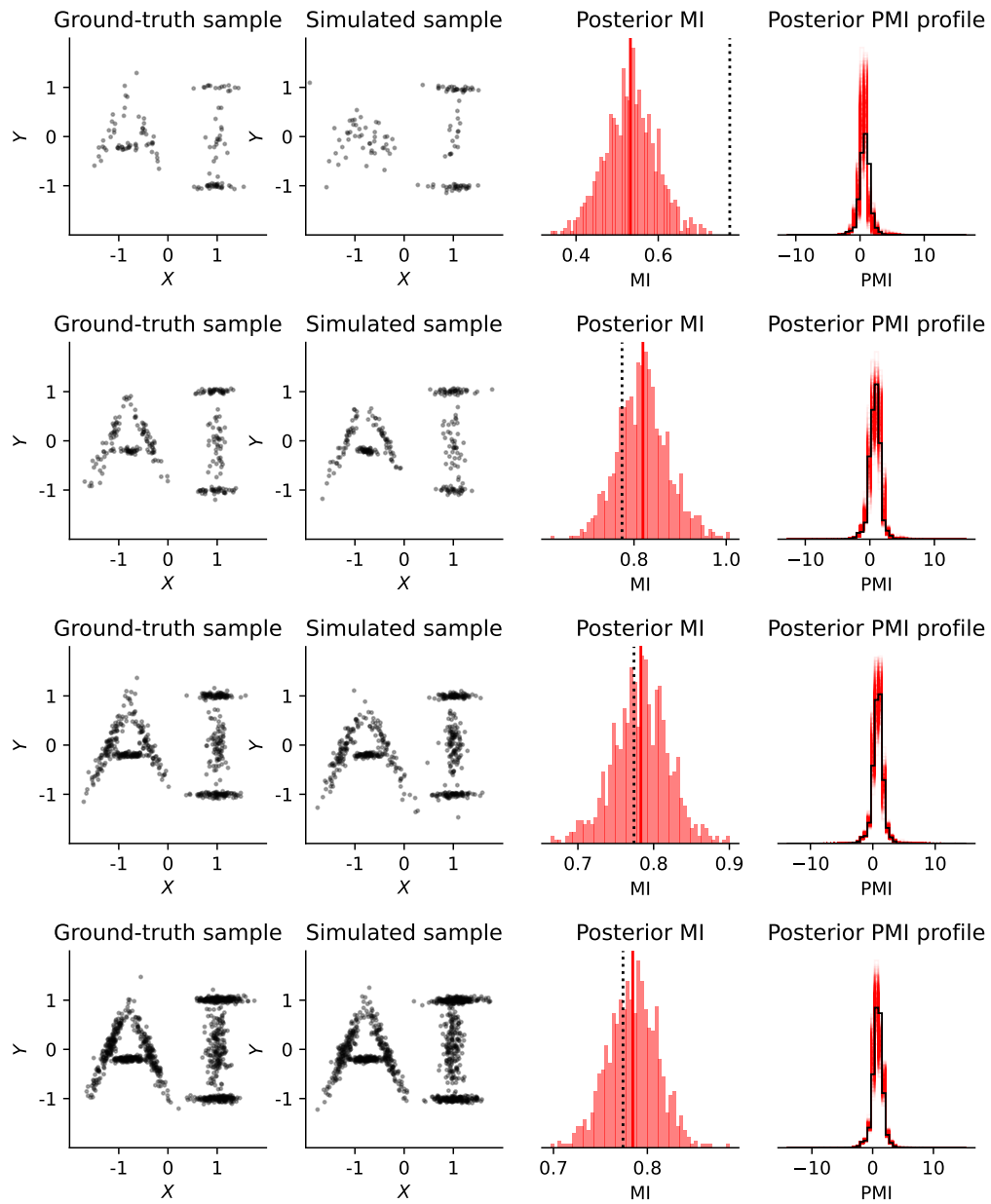


Figure 10: Gaussian mixture model fitted to the AI distribution with 125, 250, 500 and 1000 samples.

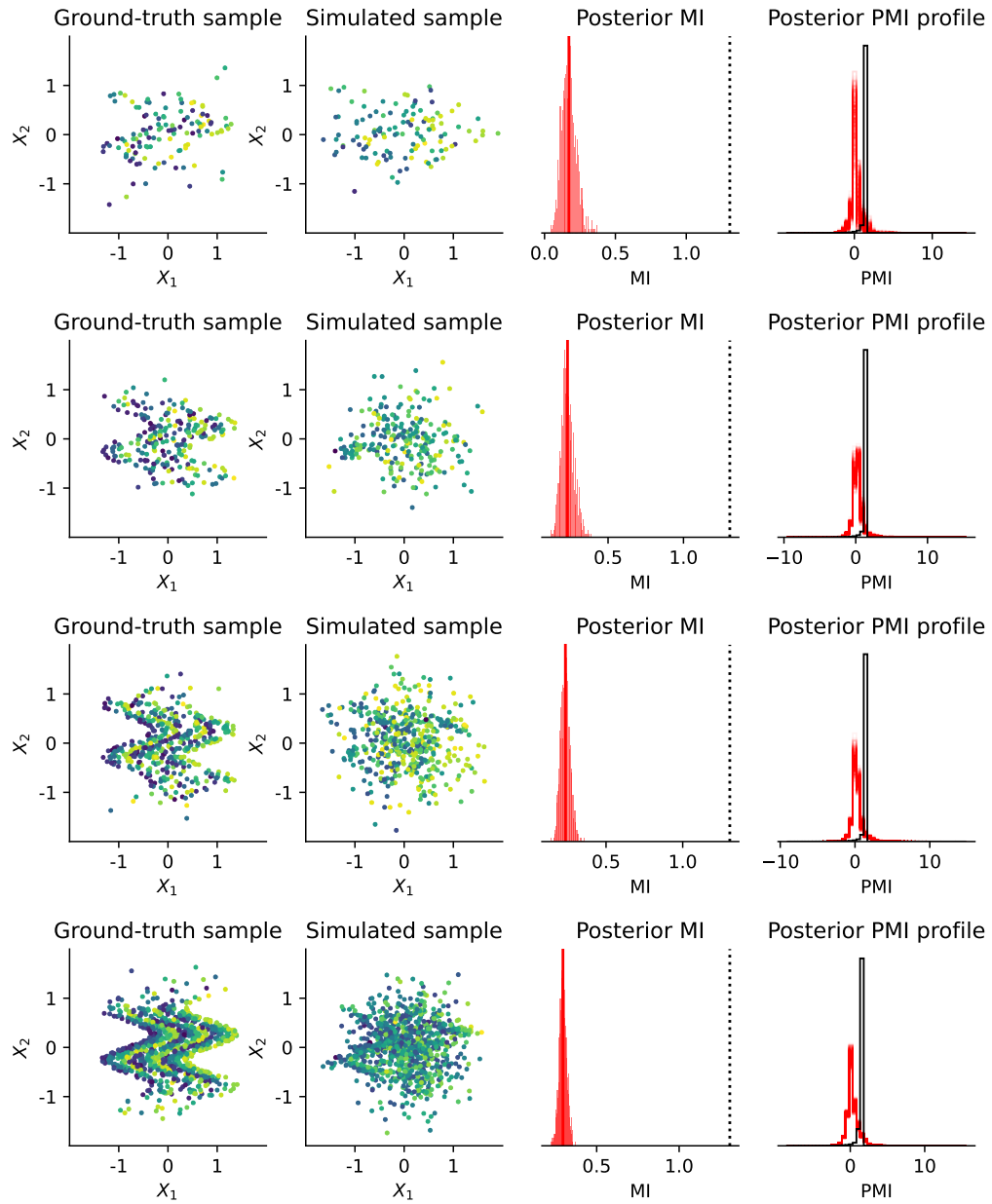


Figure 11: Gaussian mixture model fitted to the Waves distribution with 125, 250, 500 and 1000 samples.

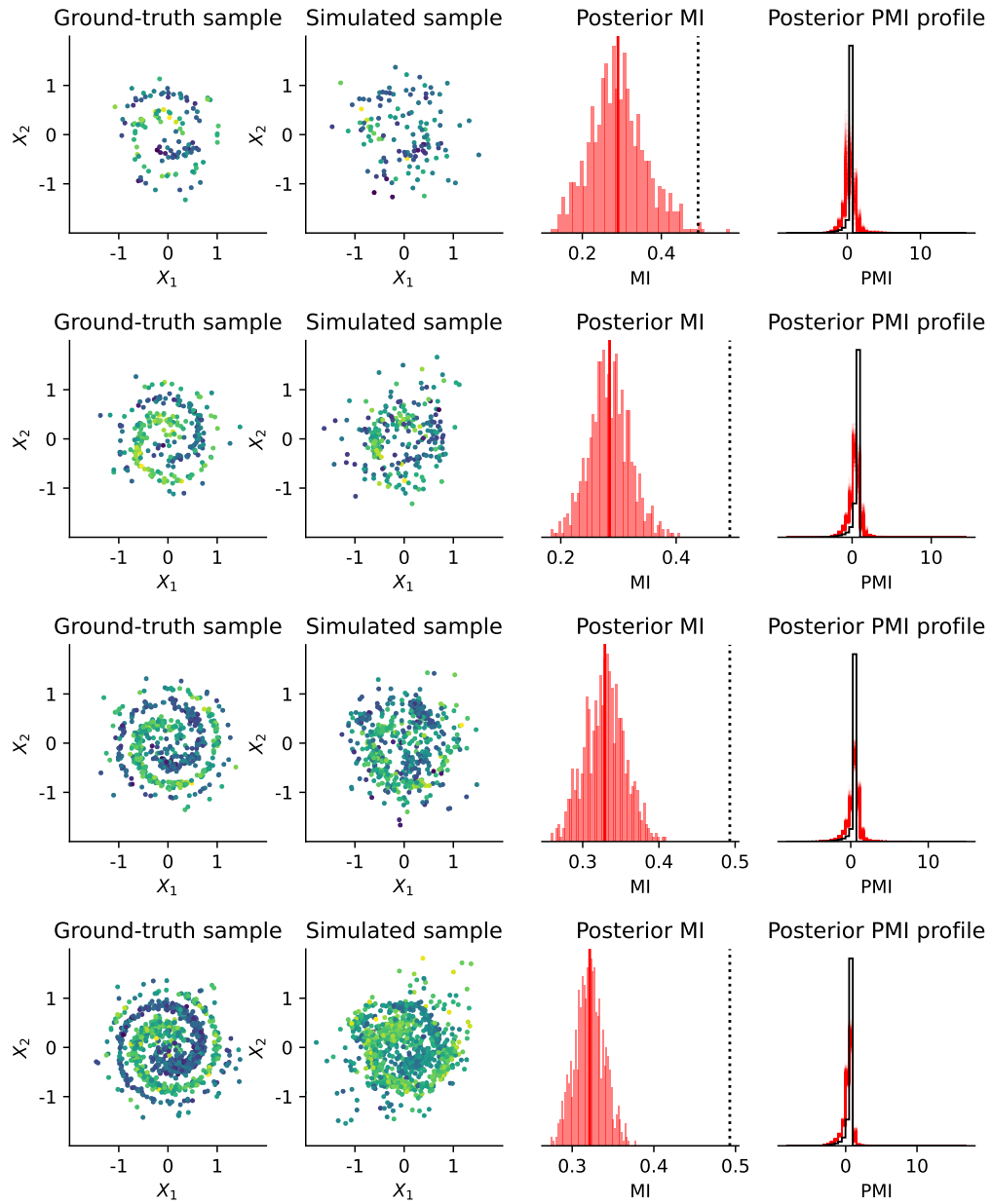


Figure 12: Gaussian mixture model fitted to the Galaxy distribution with 125, 250, 500 and 1000 samples.